Development 134, 2795-2806 (2007) doi:10.1242/dev.02868

Bi-compartmental communication contributes to the opposite proliferative behavior of Notch1-deficient hair follicle and epidermal keratinocytes

Jonghyeob Lee*, Jacob M. Basak, Shadmehr Demehri and Raphael Kopan†

Notch1-deficient epidermal keratinocytes become progressively hyperplastic and eventually produce tumors. By contrast, Notch1-deficient hair matrix keratinocytes have lower mitotic rates, resulting in smaller follicles with fewer cells. In addition, the ratio of melanocytes to keratinocytes is greatly reduced in hair follicles. Investigation into the underlying mechanism for these phenotypes revealed significant changes in the Kit, Tgfβ and insulin-like growth factor (IGF) signaling pathways, which have not been previously shown to be downstream of Notch signaling. The level of *Kitl* (*Scf*) mRNA produced by Notch1-deficient follicular keratinocytes was reduced when compared with wild type, resulting in a decline in melanocyte population. Tgfβ ligands were elevated in Notch1-deficient keratinocytes, which correlated with elevated expression of several targets, including the diffusible IGF antagonist Igfbp3 in the dermal papilla. Diffusible stromal targets remained elevated in the absence of epithelial Tgfβ receptors, consistent with paracrine Tgfβ signaling. Overexpression of Igf1 in the keratinocyte reversed the phenotype, as expected if Notch1 loss altered the IGF/insulin-like growth factor binding protein (IGFBP) balance. Conversely, epidermal keratinocytes contained less stromal Igfbp4 and might thus be primed to experience an increase in IGF signaling as animals age. These results suggest that Notch1 participates in a bi-compartmental signaling network that controls homeostasis, follicular proliferation rates and melanocyte population within the skin.

KEY WORDS: Hair follicle, Notch1, Keratinocyte, *Kitl* (*Scf*), Tgfβ, IGFBP, Mouse

INTRODUCTION

During skin organogenesis, keratinocytes and the underlying mesenchymal cells engage in reciprocal and sequential communication events that result in formation of the hair follicles, the interfollicular epidermis, the sebaceous glands and the sweat glands (Hardy, 1992; Millar, 2002; Sengel, 1976). Migratory melanocytes, and Merkel and Langerhans cells, later join in to form a community of specialized cells that together perform a unique set of physiological functions. Despite their shared origin, hair follicles and epidermal keratinocytes diverge to execute unique differentiation programs and, in the adult, replenish themselves from distinct stem cell populations (Alonso and Fuchs, 2003; Ito et al., 2005). Epidermal stem cells are restricted to the innermost (basal) layer and are the only epidermal cells that proliferate in the adult under normal circumstances (Clayton et al., 2007). Asymmetric basal cell divisions result in one cell withdrawing from the cell cycle and commencing a terminal differentiation program and a journey outwards towards the skin surface (Lechler and Fuchs, 2005). Differentiation is manifested by unique gene expression profiles that distinguish the spinous layer, granular layer and cornified layer (Fuchs and Raghavan, 2002; Jamora and Fuchs, 2002).

In the hair follicle, keratinocytes surround a teardrop-shaped core of mesenchymal cells (dermal papilla, DP) in a structure called the bulb. In contrast to the epidermis, the proliferation zone within the bulb contains many cells that are not in direct contact with a basement membrane, although the lineage-restricted stem cells do maintain contact with the DP (Legue and Nicolas, 2005). As hair matrix keratinocytes exit the cell cycle, they differentiate into several different cell layers [outer and inner root sheath, cortex and medulla (Hardy, 1992; Millar, 2002; Sengel, 1976)]. In the third week of life, murine hair follicles start to cycle (i.e. they undergo a period of destruction, rest and regeneration), which continues throughout adult life (Muller-Rover et al., 2001; Stenn and Paus, 2001). The hair shaft is actively produced during the anagen phase. During the destructive catagen phase, the bottom two thirds of each hair follicle undergoes apoptosis; only the upper third of the follicle, the stem cell niche (bulge) and the DP remain intact. Catagen lasts for approximately 3 days and is followed by the resting phase (telogen) of variable length. Subsequent entry into anagen is believed to begin when signals from the DP activate stem cells in the bulge (Stenn and Paus, 2001).

Notch signaling promotes selection of the hair fate by activated bulge stem cells (Yamamoto et al., 2003) and plays an important role in the maintenance of the follicle, in particular in the inner root sheath fate (Pan et al., 2004). Notch proteins (Notch1-4 in mice and humans) are transmembrane receptors activated by transmembrane ligands on neighboring cells (Kopan, 2002). Binding of Notch to its ligand leads to its cleavage by γ-secretase, resulting in translocation of the Notch intracellular domain (NICD) into the nucleus, where NICD binds to CSL [named from the homologous proteins CBF1 (RBPjκ, Rbpj; Mouse), Su(H) (*Drosophila*) and LAG-1 (*Caenorhabditis elegans*)]. CSL is a transcriptional repressor bound with other nuclear factors to the promoter region of particular genes. Association of NICD with CSL transiently converts CSL from transcription repressor to transcription activator, resulting in activation of downstream targets (Fryer et al., 2004; Mumm and Kopan, 2000).

Department of Molecular Biology and Pharmacology, and Division of Dermatology, Department of Medicine, Washington University School of Medicine, Box 8103, 660 South Euclid Avenue, Saint Louis, MO 63110, USA.

*Present address: Department of Developmental Biology, Stanford University School of Medicine, 279 Campus Drive, Stanford, CA 94305-5329, USA
†Author for correspondence (e-mail: kopan@wustl.edu)

Accepted 16 May 2007

In the embryonic mouse epidermis, Notch1 intracellular domain (NICD1) is ubiquitous in supra-basal keratinocytes selecting the spinous fate (Blanpain et al., 2006; Lin and Kopan, 2003; Pan et al., 2004); after birth, NICD1 is detected transiently in a small fraction of spinous cells (Y. Pan and R.K., unpublished observations). This pattern of Notch1 activation is consistent with its proposed role in suppressing proliferation and promoting differentiation via cell-autonomous modulation of targets, which might include Wnt, $p21^{cip1}$ (Cdkn1a), K1 (Krt1), K10 (Krt10), Hes1 and p63 (Trp63) (Blanpain et al., 2006; Devgan et al., 2005; Mammucari et al., 2005; Nguyen et al., 2006; Okuyama et al., 2004; Rangarajan et al., 2001). In addition, keratinocytes deficient in Notch1 are sensitive to chemical carcinogenesis, establishing Notch1 as a tumor suppressor in the epidermis (Nicolas et al., 2003). Although the role of Notch2 in the epidermis is thought to be minimal (Rangarajan et al., 2001), loss of both Notch1 and Notch2, RBPjκ or presenilins (the catalytic components of γ-secretase) results in more severe epidermal phenotypes than loss of Notch1 alone (Blanpain et al., 2006; Pan et al., 2004), indicating that Notch2 also contributes to epidermal differentiation.

The contribution of Notch signaling to follicular and epidermal homeostasis can result from both cell-autonomous and cell non-autonomous effects. Both are consistent with the role of Notch as a transcriptional modulator: the former is built on the proven ability of Notch to modulate the transcriptional landscape within keratinocytes (Blanpain et al., 2006; Devgan et al., 2005; Nguyen et al., 2006), whereas the latter posits that some of the transcripts altered by Notch encode cell surface or secreted molecules that would impact neighboring cells (Lin et al., 2000; Pan et al., 2004). In this report, we demonstrate that Notch1 plays contrasting roles in keratinocyte proliferation within the hair follicles and the epidermis, attributed largely to previously underappreciated cell non-autonomous signals. We provide evidence that Tgfβ signaling is elevated and that *Kitl* (*Scf*) expression is reduced in Notch1-deficient hair matrix keratinocytes, correlating with reduced keratinocyte mitotic rates and a reduced melanocyte population, respectively. In addition, we demonstrate that the impact on the epithelial cell cycle is not dependent on autocrine Tgfβ reception in the keratinocyte but on paracrine signaling to neighboring fibroblasts. The fibroblast, in turn, controls keratinocyte proliferation by modulating insulin-like growth factor (IGF) signaling: in the hair follicle, IGF binding protein 3 (*Igfbp3*) levels were elevated in the DP, whereas, in the epidermis, *Igfbp4* protein was reduced. Increasing the IGF/insulin-like growth factor binding protein (IGFBP) ratio by Igf1 overexpression in Notch1-deficient skin restored the cell numbers in the hair matrix. Thus, diffusible epithelial Tgfβ and stromal IGFBPs act downstream of Notch1 in a bi-compartmental signaling network within the skin. When perturbed by the loss of Notch, this paracrine loop could contribute to epidermal keratinocyte hyperproliferation in a manner analogous to the vicious cycle seen in bone metastasis (Mundy, 2002; Roodman, 2004).

MATERIALS AND METHODS

Production and analysis of single- and compound-mutant mice

The generation of $Tgfbr2^{flox}$(Yang et al., 2004), *Trp53*-null (*p53*-null) (Jacks et al., 1994), *Msx2-Cre* (Sun et al., 2000), *Ivl::Igf1* (Weger and Schlake, 2005a) and *Notch1*-conditional knockout (N1CKO) (*Msx2-Cre;*$Notch1^{flox/flox}$) (Pan et al., 2004) mice were described previously.

Notch1 Igf1 double mutants

Ivl::Igf1 females were crossed with N1CKO males, and the F1 *Msx2-Cre/+;*$Notch1^{flox/+}$*;Ivl::IGF1* male offspring were then crossed with F1 $Notch1^{flox/+}$*;Ivl::IGF1* females to produce *Msx2-Cre/+;*$Notch1^{flox/flox}$*;Ivl::IGF1* offspring.

Notch1 p53 (*Trp53*) double mutants

Female mice containing $Trp53^{-/-}$ were crossed with N1CKO males, and the male $Trp53^{-/-}$ mice were crossed with $Notch1^{flox/flox}$ females. The F1 male offspring *Msx2-Cre/+;*$Notch1^{flox/+}$*;*$Trp53^{+/-}$ were then crossed with the F1 females $Notch1^{flox/+}$*;*$Trp53^{+/-}$. The F2 offspring, *Msx2-Cre/+;*$Notch1^{flox/flox}$*;*$Trp53^{+/-}$ males and $Notch1^{flox/flox}$*;*$Trp53^{-/-}$ females, were mated to produce the compound-mutant mice *Msx2Cre/+;*$Notch1^{flox/flox}$*;*$Trp53^{-/-}$ (abbreviated to N1p53DCKO), which, along with their littermates, were used for analysis.

Notch1 Tgfbr2 double mutants

$Tgfbr2^{flox/flox}$ males and females were similarly used to generate *Msx2-Cre/+;*$Notch1^{flox/flox}$*;*$Tgfbr2^{flox/flox}$ (abbreviated to N1TGFβR2CKO) for analysis.

PCR conditions and protocols used for genotyping will be provided upon request.

Histology, in situ hybridization (ISH) and immunohistochemical analysis

To obtain stereoscopic images, 9-day-old (P9) skins in PBS were torn as strips across the caudal-rostral axis with fine forceps and photographed with an Olympus SZH10 stereo dissecting microscope. For hematoxylin and Eosin staining, ISH and immunohistochemical analyses, skins were fixed in 4% paraformaldehyde in PBS, embedded in paraffin and sectioned at 5 μm thickness. ISH was performed as described (Pan et al., 2004) with probes prepared using cDNAs generated by either reverse transcriptase (RT)-PCR or from the following sources: *Cdkn1a*, IMAGE, 3495942; *Nrarp*, IMAGE, 6439916; and *Notch1* (Kopan and Weintraub, 1993). The primer sequences for RT-PCR are available upon request. For each reaction, a corresponding sense transcript was used as a negative control. Immunohistochemical analysis was performed as described previously (Lin et al., 2000; Pan et al., 2004). For BrdU staining, animals were intraperitoneally administered with 100 μg BrdU/g body weight and sacrificed after 30 minutes. Immunohistochemical analyses with AE13, BrdU and Ki67 antibodies were performed as described (Lin and Kopan, 2003; Lin et al., 2000). Other antibodies used were Hes1 (rabbit, 1:1000; kindly provided by T. Sudo, Toray Industries, Kamakura, Japan) (Ito et al., 2000), Igfbp2 (goat, 1:200; R&D Systems, AF797), Igfbp3 (goat, 1:200; R&D Systems, AF775) and p73 (mouse, 1:1000; Labvision, ER15). For β-galactosidase (rabbit, 1:1000, 5 Prime→3 Prime) and Dct (goat, 1:200, Santa Cruz, sc-10451)-antibody staining, skins were fixed in periodate-lysine-paraformaldehyde, cryoprotected with 30% sucrose in PBS overnight, embedded in OCT and sectioned at 7 μm thickness. Sections were counterstained with DAPI.

Cell counting and progenitor cell labeling index

For hair matrix cell counting, paraffin sections were stained with DAPI and photographed under both UV and visible light. The two pictures were overlapped and nuclei located below the most proximal melanin granules were counted from each hair follicle. For each genotype, >20 hair follicles in proper longitudinal orientation were counted to calculate average and standard deviation. For progenitor cell labeling index, BrdU- and Ki67-positive cells were counted from >20 hair follicles per mouse, using three mice for each genotype. For calculating the melanocyte cell fraction, the number of Dct-positive cells was divided by the number of hair matrix cells in each follicle. The average percentage and standard deviation from >20 hair follicles per genotype was calculated. In all cases, significant differences between means were determined by the two-tailed Student's *t*-test.

TUNEL staining

Frozen unfixed dorsal skins were embedded in OCT, and 10 μm sections were prepared for TUNEL (terminal deoxynucleotide transferase dUTP-digoxigenin nick end labeling) assay. TUNEL assay was performed as described (Lindner et al., 1997). The number of TUNEL-positive cells per follicle was counted from >60 longitudinally sectioned, properly oriented follicles from each individual [anagen-deleted Notch1 (anN1) and embryo-deleted Notch1 (emN1) follicles from N1CKO mice at P9; wild-type follicles at P9 and P16], and three different individuals were used. Statistical significance was determined by the two-tailed Student's *t*-test.

Isolation of hair bulbs and epidermis, total RNA extraction, and microarray analyses

For hair bulb isolation, fresh P9 skin samples were immediately immersed in RNAlater (Ambion, TX) and individual hair follicles were collected using a fine tungsten needle and precisely cut with a 26G syringe needle (Becton Dickinson and Company, NJ) at the level twice the distance between the tip of the bulb and the melanin granules (Fig. 3A). For epidermis preparation, a patch of P9 dorsal skin was harvested and flash-frozen with dry ice, and the epidermis was isolated by scraping it off the skin using a cold scalpel. Isolated hair bulbs and epidermis samples were then subjected to total RNA isolation using QIAGEN RNeasy micro kit (QIAGEN Sciences, MD) according to the manufacturer's protocol. For hair bulb microarray analyses, 50-100 ng of total RNA was collected from emN1 and anN1 follicles isolated from the same N1CKO mouse (total of two mice) and from two wild-type littermates. After double-round amplification/labeling procedures, the cRNA products were hybridized to Affymetrix MOE430v2 chips. All protocols were conducted at the Washington University Genechip Facility (http://www.siteman.wustl.edu/internal.aspx?id=238). Affymetrix microarray suite 5.0 and dChip software (http://www.dchip.org) were used for expression profile comparisons and GO (gene ontology)-based classification. The data discussed in this publication have been deposited in NCBIs gene expression omnibus (GEO, http://www.ncbi.nlm.nih.gov/geo/) and are accessible through GEO Series accession number GSE6867. Ingenuity and David2 (http://niaid.abcc.ncifcrf.gov/) were used for pathway analyses.

cDNA preparation and quantitative reverse transcriptase (qRT)-PCR

Total RNA from hair bulbs and epidermis was used for cDNA preparation using QIAGEN Sensiscript RT kit (QIAGEN Sciences, MD) according to the manufacturer's protocol. The cDNA was amplified with SYBR-Green PCR Master Mix (Applied Biosystems, CA) and gene-specific exon-exon junction-spanning primers using the ABI7700 sequence detection system (Applied Biosystems, CA) or the MyIQ iCycler (Bio-Rad, CA). Normalizations across samples were performed using hypoxanthine guanine phosphoribosyl transferase 1 (*Hprt1*) or glyceraldehyde-3-phosphate dehydrogenase (*Gapdh*) primers. The differences between samples and controls were calculated using the comparative C_T ($2^{-\Delta\Delta CT}$) method. The histograms in the figures show the mean±s.e.m. of two or three independent experiments for hair follicles and of five independent experiments for epidermal samples, each of which was performed in triplicate. All qRT-PCR primers were tested for the presence of non-specific primer dimers and for linear amplification. The identity of the qRT-PCR amplicons was validated by DNA sequencing or restriction-enzyme digestion of the amplicon. Primer sequences and qRT-PCR conditions are available upon request.

Immunoblotting

Frozen epidermal samples were immediately lysed in NP40 lysis buffer (1% NP-40, 150 mM NaCl, 10% glycerol, 1 mM EDTA, 20 mM Tris, pH 8.0) containing protease and phosphatase inhibitors and analyzed by SDS-PAGE/western blotting. The following primary antibodies were used: α-tubulin (mouse, 1:1000; Sigma-Aldrich B-5-2), cyclin D1 (rabbit, 1:1500; Santa Cruz sc-718), Igfbp4 (rabbit, 1:5000; kindly provided by Chernausek, Cincinnati Children's Hospital, Cincinnati, OH), p15 (Cdkn2b; rabbit, 1:200; Santa Cruz sc-612), p21 (mouse, 1:100; Santa Cruz sc-6246) and anti-Tgfβ2 (rabbit, 1:200; Santa Cruz sc-90). Western blot quantification was performed using Quantity One software (Bio-Rad Laboratories, CA). The histograms in the figures show mean±s.e.m. of two or three independent epidermal lysates per genotype.

RESULTS

The bulbs of Notch1-deficient hair follicles contain fewer keratinocytes than wild type

Conditional deletion of Notch1 in *Msx2Cre;Notch1*$^{flox/flox}$ (abbreviated to N1CKO) mice produced chimeric skin with two different patterns of gene loss in hair follicles, previously described as anagen-deleted (abbreviated to anN1) and embryo-deleted (abbreviated to emN1) (Fig. 1A) (Pan et al., 2004). As the names imply, emN1 epidermis and follicles are derived from cells that experienced a pulse of Cre activity at embryonic day (E)9.5 and thus lack Notch1 from that point onwards. Conversely, anN1 follicles express Cre recombinase in the mid-bulb region a few days after the start of the growth phase (anagen); Notch1 is thus only removed in the upper bulb (Fig. 1A). We observed that emN1 follicles were substantially shorter than anN1 or wild-type follicles (Fig. 1B,C). Because anN1 follicles were wild type in appearance, we concluded that growth-related Notch1 functions are required in the proximal, actively proliferating matrix during hair morphogenesis (Fig. 1B,C) (Pan et al., 2004).

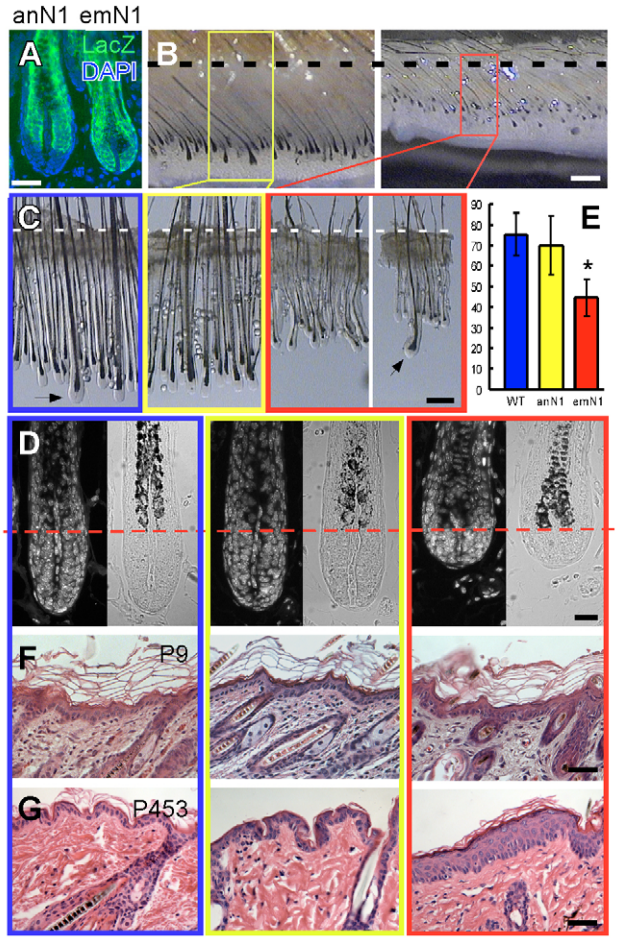

Fig. 1. Notch1 loss leads to reduced cell numbers in hair follicles but to an expansion in the number of epidermal keratinocytes. (**A**) β-galactosidase (*lacZ*, green) immunohistochemistry on *Msx2Cre;Notch1*$^{flox/flox}$*;Rosa26R/+* skin. Note that β-galactosidase staining displays the area of Notch1 deletion. (**B**) Stereoscopic side view of anagen-deleted Notch1 (anN1; left) and embryo-deleted Notch1 (emN1; right) skin at 9 days of age (P9). (**C**) Stereoscopic view magnified from the images shown in B after dissection. Wild type, left (blue box); anN1, middle (yellow box); emN1, right (red box). Arrows indicate guard hairs. (**D**) Histological view of the follicles shown in B and C. The different genotypes are designated as in C. Nuclei were stained with DAPI. (**E**) Average number of hair matrix cells (below the red line in D) per hair follicle. **P*<0.00001. Error bars represent s.d. (**F**,**G**) Hematoxylin and Eosin staining of P9 (F) and P453 (G) skin. Notice the epidermal hyperplasia in older emN1 skin (G). Scale bars: 50 μm in A; 300 μm in B; 200 μm in C; 20 μm in D; 40 μm in F,G.

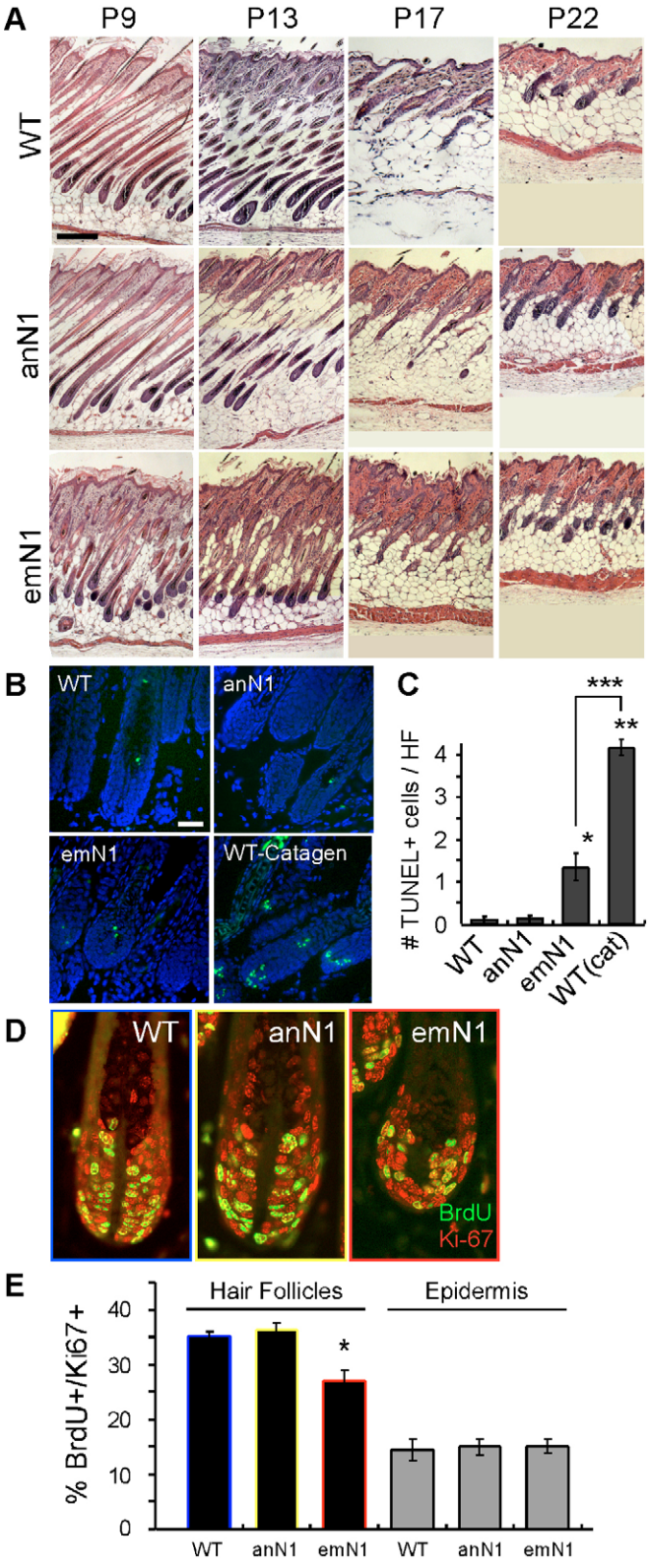

Fig. 2. Notch1 loss causes decreased mitotic rates and a slight increase in apoptosis, but not acceleration in catagen onset. (**A**) Hematoxylin and Eosin staining of anagen-deleted Notch1 (anN1), embryo-deleted Notch1 (emN1) and wild-type (WT) skin at 9 days (P9), P13, P17 and P22 old. Note that hair cycling was not altered in Notch1-deficient hair follicles. (**B**) TUNEL staining of emN1 and anN1 follicles (P9), and of wild-type hair follicles [P9 and P16 (catagen)]. (**C**) Average number of TUNEL-positive cells per hair follicle in each genotype shown in B. **P*<0.05 for both wild type versus emN1 and anN1 versus emN1; ***P*<0.05 for both wild type versus wild type (catagen) and anN1 versus wild type (catagen); ****P*<0.005. (**D**) Immunofluorescence staining of BrdU (green) and Ki67 (red). (**E**) Progenitor labeling index of anN1, emN1 and wild-type hair follicles and epidermis. **P*<0.01 for anN1 versus emN1 and wild type versus emN1. Error bars represent s.d. Scale bars: 200 μm in A; 20 μm in D.

Closer inspection of hair bulbs at postnatal day (P)9 revealed that the portion below the most-proximal melanin granules (marked by a dashed red line in Fig. 1D) was shorter in the emN1 follicles compared with wild-type or anN1 follicles (Fig. 1D). Cell size in all genotypes was not altered. Instead, fewer cells were detected in Notch1-deficient follicles: emN1 hair follicles had only 44.69±8.92 cells, whereas wild-type (75.32±10.30) and anN1 (69.86±14.17) hair follicles had nearly twice as many cells (Fig. 1E). Notch1-deficient epidermis did not display any observable hyperplasia at this age, but the epidermis of older mice did (Fig. 1F,G) (Nicolas et al., 2003; Rangarajan et al., 2001). We thus conclude that, in contrast to the epidermis, in which the number of Notch1-deficient epidermal keratinocytes increases as mice age (Nicolas et al., 2003; Rangarajan et al., 2001), fewer Notch1-deficient keratinocytes formed the hair bulb. Therefore, Notch1 loss leads to differential effects on related keratinocyte populations.

Notch1-deficient hair matrix cells have decreased mitotic rates

During catagen, hair bulbs involute and regress quickly (within 3-4 days) via a combination of cell cycle arrest and apoptotic cell death (Dry, 1926; Lindner et al., 1997; Muller-Rover et al., 2001; Weedon and Strutton, 1981). One trivial explanation for reduced keratinocyte numbers in emN1 bulbs compared with wild type is accelerated catagen onset, as observed in mice with global epithelial deletion of Notch1 [*K14-Cre; Notch1*$^{flox/flox}$ and *K5-Cre*^{ERT}*; Notch1*$^{flox/flox}$ (Vauclair et al., 2005)]. To determine whether reduced cell numbers in emN1 hair bulbs reflected early catagen onset at P9, we examined emN1 skin at P9, P13, P17 and P22 (Fig. 2A). If catagen had started at P9, the lower two thirds of the follicles would have been lost by P13. Instead, characteristic follicular catagen destruction was not detected before P17 in all genotypes, indicating that Notch1-deficient skin in N1CKO mice did not exhibit accelerated entry into catagen (Fig. 2A).

Early catagen (stage II) follicles contain, on average, four or more TUNEL-positive cells (Lindner et al., 1997) (Fig. 2B,C). Although we observed a few Notch1-deficient follicles containing more than two TUNEL-positive cells, which is characteristic of the morphologically distinct catagen stage I (Muller-Rover et al., 2001), more than 40% of emN1 hair follicles lacked TUNEL-positive cells. Moreover, the average number of TUNEL-positive cells was significantly lower in emN1 follicles at P9 compared with that seen at P16, at which point, based on morphology, the cells are already undergoing catagen (1.34 versus 4.18, respectively; *P*<0.005; Fig. 2C). Given that no further morphological changes were detected, we concluded that the increased apoptotic cell death in emN1 follicles at P9 did not indicate catagen onset nor could it explain the reduced cell number seen in TUNEL-negative emN1 hair follicles.

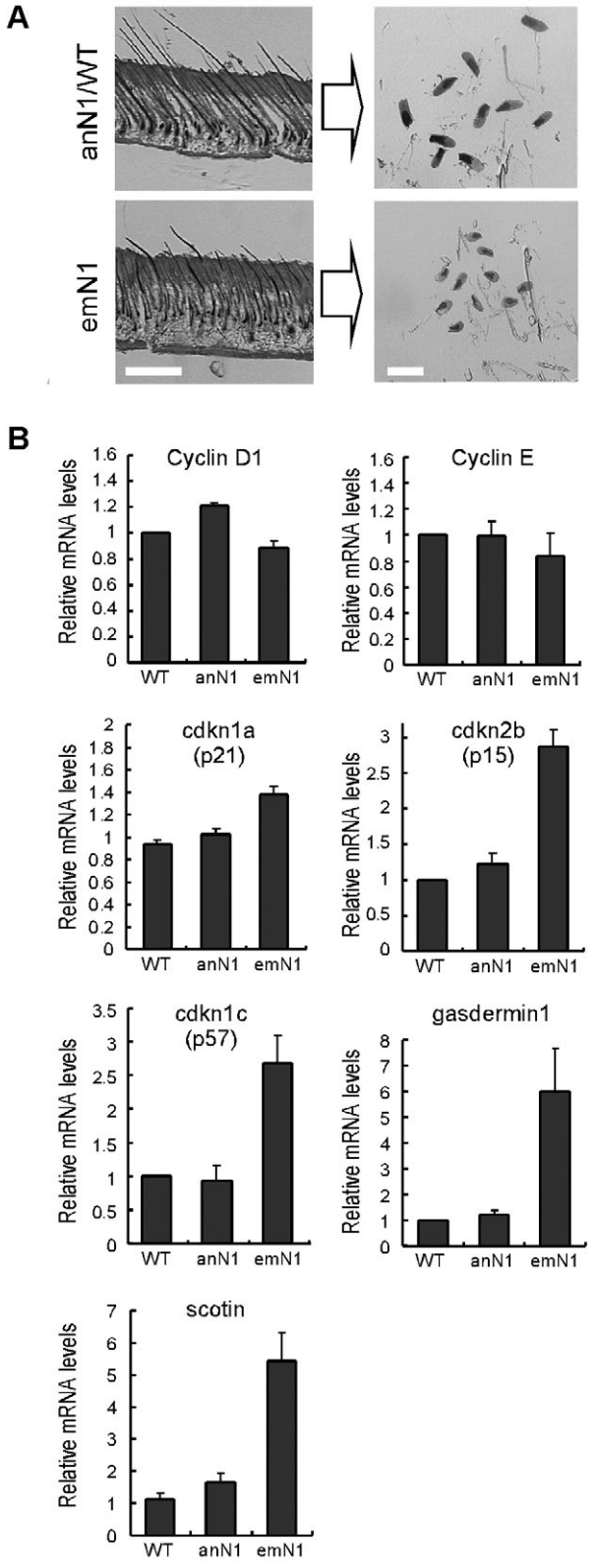

Fig. 3. Reduced mitotic rates in hair follicles correlates with elevated expression of cytostatic and proapoptotic genes. (**A**) Microdissection of hair bulbs from embryo-deleted Notch1 (emN1) or anagen-deleted Notch1 (anN1)/wild-type (WT) follicles (grouped for this image because they have the same morphology). (**B**) Quantitative reverse transcriptase (qRT)-PCR of G1 cyclins, cyclin kinase inhibitors (CKIs; *Cdkn1a*, *Cdkn2b* and *Cdkn1c*), gasdermin 1 and *Scotin* using total RNA isolated from the microdissected samples shown in A. Error bars represent s.e.m. Scale bars: (A, left) 100 μm; (A, right) 200 μm.

Another possible explanation for the lower cell numbers in emN1 follicles is a reduced proliferation rate. To examine mitotic rates at P9, we labeled mitotic cells with Ki67 (Fig. 2D, red) and S-phase cells by BrdU-incorporation (Fig. 2D, green) following a 30-minute BrdU pulse-label (Chenn and Walsh, 2002). The proportion of S-phase cells in the cycling population (BrdU+/Ki67+) was determined for the hair follicles and the epidermis of mutant and wild-type mice. Interestingly, emN1 hair follicles displayed a reduced progenitor-labeling index (27.07±1.99%) compared with anN1 (36.26±1.33%) and wild-type (35.28±0.71%) follicles (Fig. 2E), which correlated with the cell numbers in these follicles. Therefore, the lower cell numbers within Notch1-deficient hair bulbs is probably due to a delayed cell cycle, with a small contribution from increased apoptotic cell death. Interestingly, P9 epidermal keratinocytes did not display any difference in the progenitor-labeling index (Fig. 2E), indicating that the proliferation defect in epidermal keratinocytes is progressive, evident only as the animals age.

Notch1-deficient hair follicles contain elevated levels of transcripts encoding cytostatic and proapoptotic proteins

The length of the G1 phase in mammalian cells can vary, whereas the lengths of the S and G2+M phases remain relatively unchanged (Chenn and Walsh, 2002; DiSalvo et al., 1995; Malkinson and Keane, 1978). The reduced mitotic rate in emN1 follicles might be attributable to changes in G1 length or in the G1/S checkpoint, perhaps due to decreased expression/stability of G1 cyclins or increased levels of cyclin kinase inhibitors (CKIs) (Mainprize et al., 2001; Massague, 2004; Sherr and Roberts, 1999). To address the molecular mechanism underlying the lowered mitotic index and increased apoptosis seen in Notch1-deficient hair follicles, we performed microarray analyses on total RNAs extracted from a pool of approximately 100 micro-dissected emN1 and anN1 hair bulbs (isolated from the same N1CKO mouse) as well as wild-type hair bulbs isolated from a littermate (Fig. 3A). emN1 and anN1 samples from one animal were compared to each other and to a wild-type littermate in silico; differences present in two biological duplicates were then compiled to produce a 'proximal bulb' signature (the precise comparison matrix of the six samples is available upon request). Genes altered in the emN1 bulb but not in the anN1 bulb or in the anN1/wild-type comparison were subjected to GO (gene ontology)-based classification and Ingenuity pathway analysis. We identified 47 genes altered in Notch1-deficient hair matrix that are involved in cell growth, cell cycle, cell proliferation or programmed cell death (see Table S1 in the supplementary material).

Microarray analysis and quantitative reverse transcriptase (qRT)-PCR revealed that transcription of the CKIs *Cdkn1a* (encoding $p21^{Cip1}$), *Cdkn2b* (encoding $p15^{INK4b}$) and *Cdkn1c* (encoding $p57^{Kip2}$) was increased upon Notch1 loss, whereas mRNA expression of the G1 cyclins (cyclin D1 and cyclin E) did not change (Fig. 3B and see Table S1 in the supplementary material). In addition, the expression of *Gsdm1* (gasdermin 1), thought to promote cell cycle arrest in keratinocytes and in the gastrointestinal

tract (Lunny et al., 2005; Saeki et al., 2000), was significantly increased (Fig. 3B and see Table S1 in the supplementary material). Moreover, the mRNA level of a proapoptotic gene, *Scotin*, was also significantly induced upon Notch1 loss (Fig. 3B), consistent with the observed increase in apoptosis (Fig. 2C). These data are consistent with the hypothesis that loss of Notch1 affected the length of the G1 phase via the increased expression of cytostatic genes and caused a slight increase in apoptosis due to elevated levels of proapoptotic gene expression in follicular keratinocytes.

The impact of Notch1 loss is not mediated via p53 family members

The cytostatic and proapoptotic transcripts elevated in Notch1-deficient follicles include the p53 family targets *Cdkn1a*, *Scotin* (Fig. 3B) (Harms and Chen, 2005; Rossi et al., 2004; Terrinoni et al., 2004) and *Igfbp3* (Fig. 5A, described in detail below). Members of the p53 family are known regulators of G1/S arrest and of apoptosis (Bartek and Lukas, 2001; Massague, 2004; Moll and Slade, 2004). In the epidermis, loss of Notch1 resulted in elevated p63 levels (Nguyen et al., 2006), which in turn contributed to proliferation at the expense of differentiation. *Trp63* (encoding p63) transcripts were slightly elevated in Notch1-deficient follicles (Fig. 4A), whereas transcripts of *Trp73* (encoding p73) were greatly elevated (Fig. 4A). In wild-type mice, p73 expression was restricted to a subset of lineage-restricted stem cells adjacent to the DP (Fig. 4B). In the absence of *Notch1*, p73 expression extended to inner root sheath and outer root sheath cells (Fig. 4B), indicating that Notch1 or its targets might negatively regulate p73 expression. However, this expression pattern did not overlap with the expression domain of any of the p53 family targets (Fig. 4B, Fig. 5B and Fig. 8B). Moreover, p73-positive cells were actively cycling, as evident from BrdU-incorporation studies (compare Fig. 2D with Fig. 4B).

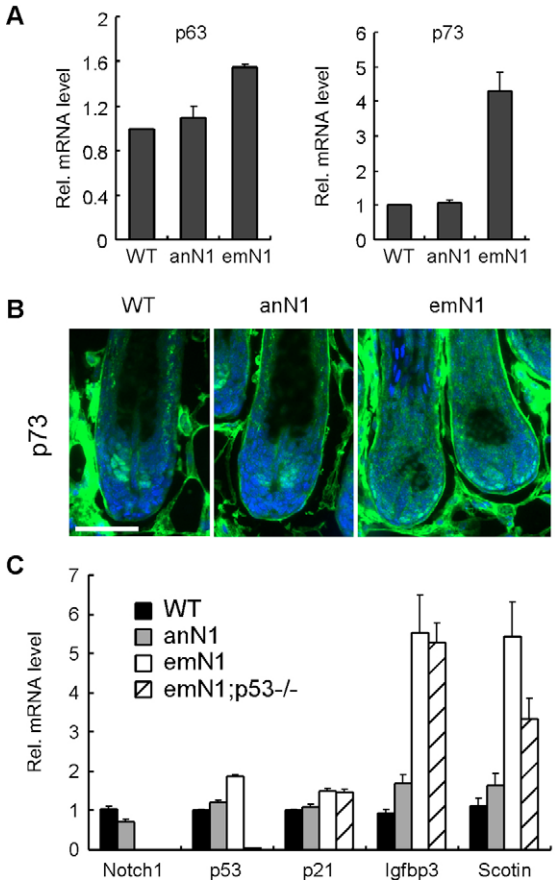

Fig. 4. p53 family members do not contribute to the Notch1-deficient follicular phenotype. (**A**) Quantitative reverse transcriptase (qRT)-PCR of p63 and p73. (**B**) Immunohistochemistry of p73 in hair follicles of anagen-deleted Notch1 (anN1), embryo-deleted Notch1 (em-N1) and wild-type (WT) littermates. (**C**) qRT-PCR with *Notch1*, *Trp53* (*p53*) and p53 target genes [*Cdkn1a* (p21), *Igfbp3* and *Scotin*] using total RNA from the hair bulbs of the genotypes specified (emN1;p53–/– indicates *Msx2Cre;Notch1$^{flox/flox}$;Trp53$^{-/-}$*). Note the sustained increase in *Scotin* and *Igfbp3* expression in the absence of p53. Error bars represent s.e.m. Scale bar: 50 μm.

Notch loss can lead to a reduction in p53 activity in neurons or cultured cells (Huang et al., 2004; Yang et al., 2004). To explore whether changes in p53 accumulation contributed to the *Notch1$^{-/-}$* phenotype, or enhanced it, we crossed our N1CKO mice with p53-deficient mice. Skin morphology and histology of compound homozygous mice (*Msx2-Cre;Notch1$^{flox/flox}$;Trp53$^{-/-}$*) were indistinguishable from that of N1CKO (see Fig. S1 in the supplementary material). Importantly, the mRNAs of the p53 family targets *Igfbp3*, *Cdkn1a* and *Scotin* did not change in compound *Msx2-Cre;Notch1$^{flox/flox}$;Trp53$^{-/-}$* hair follicles (Fig. 4C). Therefore, we conclude that none of the p53 family members contribute significantly to the *Notch1$^{-/-}$* phenotype in the hair follicle.

Altered IGF signaling in Notch1-deficient hair follicles

Our microarray analyses revealed that transcripts for IGF signaling modulators (Igfbp2, Igfbp3 and Igfbp4) are elevated in Notch1-deficient hair bulbs, as is the IGF receptor (Fig. 5A and see Table S1 in the supplementary material). Indeed, pathway analysis of transcripts altered in emN1 relative to wild-type follicles confirmed that the vast majority of possible protein networks were anchored around IGFBPs (data not shown). IGF signaling promotes cell proliferation by reducing the length of the G1 phase (Edmondson et al., 2003), the inverse of the phenotype we observed in Notch1-deficient hair follicles (Fig. 2). Diffusible IGFBPs antagonize the mitogenic (Baserga et al., 1997; Firth and Baxter, 2002) and anti-apoptotic (Butt et al., 1999; Resnicoff and Baserga, 1998) activity of Igf1 by sequestering it from its receptors (Edmondson et al., 2003; Firth and Baxter, 2002).

To determine whether changes in IGF signaling underlie the *Notch1$^{-/-}$* phenotype, we attempted to confirm the observed changes in IGFBP expression in the microarray at the tissue level. Igfbp2 expression was detected in the nuclei of hair matrix cells, and no change in its distribution was evident at the protein level in Notch1-deficient hair follicles (Fig. 5B). Strikingly, whereas *Igfbp3* mRNA and protein were undetectable in wild-type hair follicles, their expression was evident in DP fibroblasts but not the keratinocytes of Notch1-deficient hair follicles (Fig. 5B).

Igfbp3 is a diffusible molecule and its ectopic expression in hair follicles leads to decreased hair length and bulb volume (Weger and Schlake, 2005b), a phenotype strikingly similar to Notch1-deficient hair follicles (Figs 1 and 2). Conversely, ectopic expression of Igf1 promotes hair growth and follicular elongation (Su et al., 1999a; Su et al., 1999b; Weger and Schlake, 2005a). Importantly, mice overexpressing both Igf1 and Igfbp3 are normal (Weger and Schlake, 2005a), indicating that IGF/Igfbp3 balance is an important regulator of follicular keratinocyte proliferation.

To determine whether Igf1 overexpression (and thus a higher IGF/IGFBP ratio) can rescue Notch1-deficient hair follicles, we generated *Msx2-Cre;Notch1$^{flox/flox}$;Ivl::IGF1* mice (Weger and

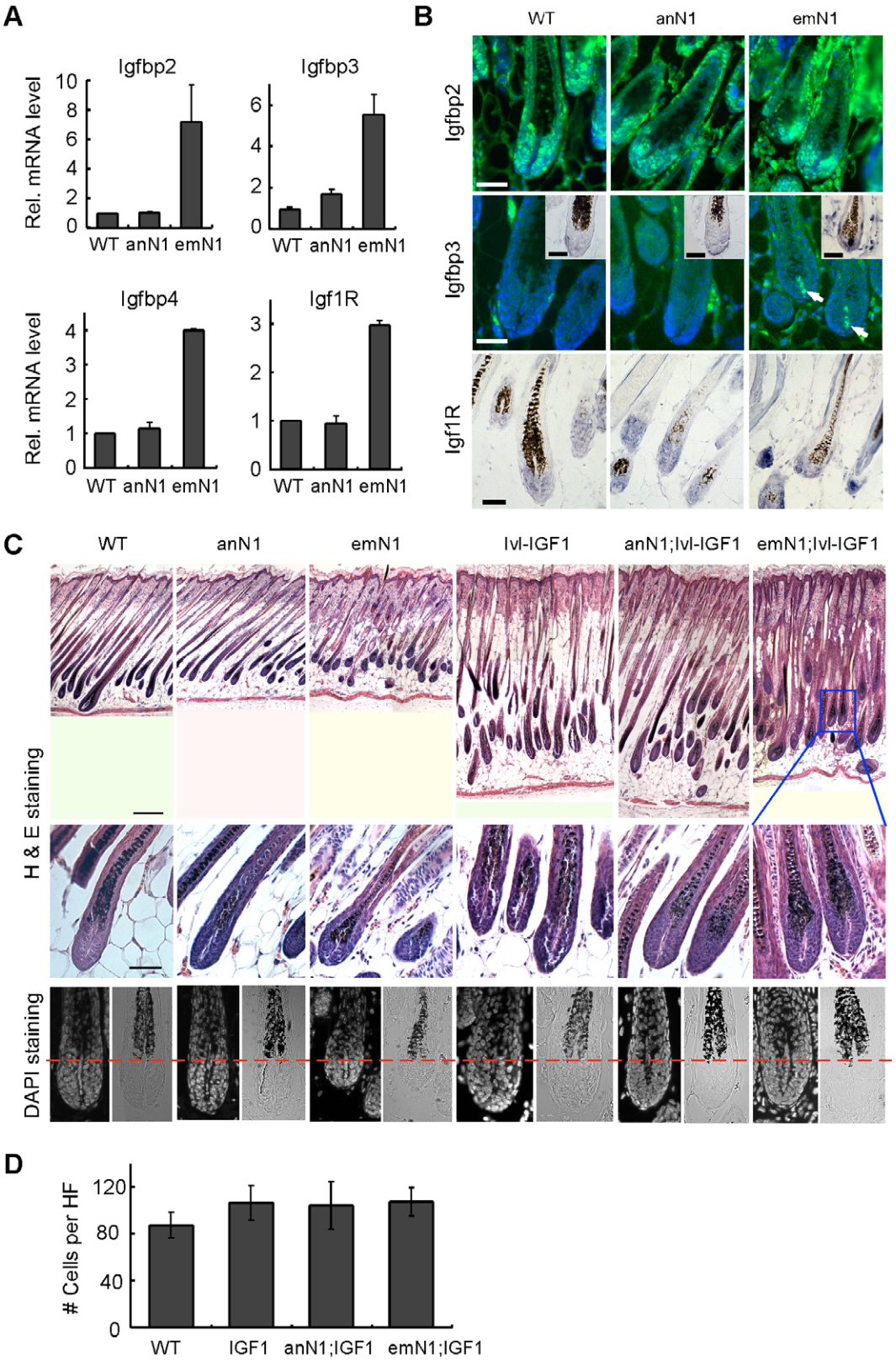

Fig. 5. Altered IGF/IGFBP equilibrium in the hair matrix of Notch1-deficient hair follicles. (**A**) Quantitative reverse transcriptase (qRT)-PCR of IGF signaling components. Error bars represent s.e.m. (**B**) Immunohistochemistry (Igfbp2 and Igfbp3) and in situ hybridization (Igf1R and insets for Igfbp3) of IGF signaling components on hair follicles. DAPI was used to label nuclei during antibody staining. Arrows indicate dermal papilla (DP)-specific Igfbp3 immunoreactivity. Note the mRNA and protein expression of *Igfbp3* in the DP, in which Notch1 is not expressed. (**C**) Histological comparisons of the hair follicles from the genotypes specified. Note that the matrix size is restored in embryo-deleted Notch1 (emN1);Ivl::Igf1 follicles. (**D**) Average number of hair matrix cells (below the red line in C) per hair follicle. Error bars represent s.d. anN1, anagen-deleted Notch1. Scale bars: 40 μm in B; 200 μm [skin hematoxylin and Eosin (H&E) staining] and 50 μm (follicular H&E and DAPI staining) in C.

Schlake, 2005a) and analyzed the morphology of their hair follicles at P9. The cell numbers in Notch1-deficient Igf1-expressing hair follicles increased (Fig. 5C,D), indicating that an imbalance between IGF ligand and IGFBPs was indeed a contributing factor to the phenotype of Notch1-deficient follicles.

As described above, a change in protein expression in one compartment (Notch1 loss in keratinocytes) led to a change in another compartment (Igfbp3 gain in the DP). It is important to note that dermal fibroblasts and the DP did not experience *Msx2-Cre* activity (as evident from the lack of *lacZ* expression in *Msx2-*

Cre;Rosa26R skin; Fig. 1A and data not shown). In addition, they did not express *Notch1* mRNA or protein (Fig. 8 and see Fig. S6 in the supplementary material), and were even separated from Notch1-expressing cells by a basement membrane and a layer of keratinocytes lacking Notch1 proteins. Therefore, a longer G1 phase in Notch1-deficient matrix keratinocytes probably involves a cell non-autonomous mechanism (e.g. elevation of *Igfbp3* in the DP), perhaps in combination with a cell-autonomous mechanism (e.g. elevated expression of the *Igfbp2*, cytostatic and proapoptotic genes). We again turned to the array information in search of candidate molecules that can participate in bi-compartmental communication.

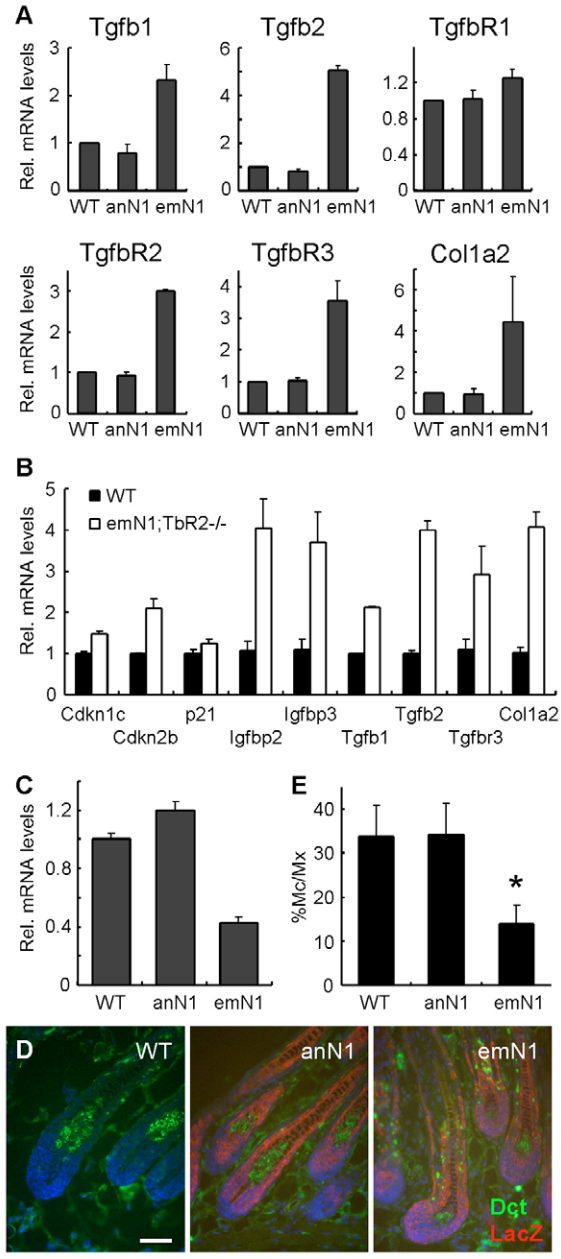

Fig. 6. Notch1 loss alters the expression of the diffusible ligands Kitl and Tgfβ. (**A**) Quantitative reverse transcriptase (qRT)-PCR of Tgfβ signaling components and a downstream target (Col1a2). (**B**) qRT-PCR of the genes specified using *Notch1*- and *Tgfbr2*-deficient hair bulbs. (**C**) qRT-PCR of *Kitl* using hair follicle total RNA from the genotypes specified. (**D**) Immunohistochemical staining of wild-type and *Msx2Cre;Notch1*$^{flox/flox}$*;Rosa26R/+* mice with Dct (green) and β-galactosidase (*lacZ*, red). Nuclei were stained with DAPI. Note that melanocytes (Dct positive) do not show β-galactosidase staining. (**E**) The ratio of melanocytes (Dct positive) to the matrix cells in each follicle was obtained from the different genotypes specified. Notice the reduced number of melanocytes in Notch1-deficient hair follicles (*P<0.0001 in both WT versus em-N1 and an-N1 versus em-N1). Error bars represent s.e.m. (A-C) and s.d. (D). Scale bar: 50 μm.

Changes in epithelial Tgfβ ligands lie downstream of Notch1 and might contribute to the skin phenotype

Components of the Tgfβ signaling pathway, which has been shown to induce IGFBPs and CKIs and thus promote G1 arrest (Firth and Baxter, 2002; Jetten et al., 1986; Moustakas et al., 2002), were also altered in N1CKO skin. Transcription of the ligands *Tgfb1* and *Tgfb2*, the receptor *Tgfbr2* [itself a target of Tgfβ signaling (Cui et al., 1995)], the co-receptor *Tgfbr3* (Brown et al., 1999), as well as the Tgfβ targets *Col1a2* (Inagaki et al., 1994) and *Thbs1*, were all elevated in the emN1 hair bulb (Fig. 6A and see Table S1 in the supplementary material). The ligands Tgfβ1 and Tgfβ2 and the receptors TgfβRI and TgfβRII were all expressed in the hair follicle (see Fig. S2 in the supplementary material) (Paus et al., 1997). These receptors were also expressed in the DP (see Fig. S2 in the supplementary material), whereas *Col1a2* was specifically expressed in dermal fibroblasts (Zheng et al., 2002). Because Tgfβ-mediated signaling can act both as an autocrine and a paracrine signal, this pathway is capable of activating the transcription of *Igfbp2* in keratinocytes (Moustakas et al., 2002; Scandura et al., 2004), as well as that of *Igfbp3* in neighboring cells (Guo et al., 1995; Martin and Baxter, 1991).

To determine whether autocrine reception of Tgfβ plays a role in hair matrix homeostasis, we removed the essential type II receptor *Tgfbr2* in all Notch1-deficient keratinocytes by generating *Msx2Cre;Tgfbr2*$^{flox/flox}$ (termed TgfβR2CKO) and *Msx2Cre;Notch1*$^{flox/flox}$*;Tgfbr2*$^{flox/flox}$ (termed N1TgfβR2CKO) mice. Only dermal fibroblasts and DP cells in these compound mice retained the ability to respond to Tgfβ ligands via TgfβRII, yet the skin of TgfβR2CKO mice was indistinguishable from wild type (data not shown and see Fig. S3 in the supplementary material). Importantly, hair follicles from N1TgfβR2CKO and N1CKO mice were morphologically identical, and qRT-PCR analysis confirmed that the expression of *Tgfb1*, *Tgfb2*, *Tgfbr3*, *Igfbp2*, *Igfbp3*, *Col1a2* and CKIs remained elevated in N1TgfβR2CKO emN1 hair bulbs (Fig. 6B). These observations indicate that: (1) even though a block in Tgfβ signaling in bulb keratinocytes has not been demonstrated, TgfβRII-mediated Tgfβ signals do not regulate the proliferation/apoptosis of hair matrix keratinocytes cell-autonomously; and (2) elevated *Igfbp2* or CKI mRNA levels might not be a consequence of autocrine Tgfβ signaling in the hair matrix. Collectively, our results described thus far are consistent with the hypothesis that *Notch1* regulates hair matrix proliferation both autonomously, by preventing expression of proapoptotic and cytostatic genes, and non-autonomously, by establishing a bi-compartmental feed-back loop. Loss of *Notch1* in transit amplifying keratinocytes induced the expression of Tgfβ ligands, which were recognized by DP cells. As a possible consequence of Tgfβ signaling, diffusible Igfbp3 was produced in DP cells to inhibit follicular IGF signaling and suppress the proliferation of follicular keratinocytes.

Bi-compartmental signals also impact melanocyte populations

In silico comparison of transcripts from Notch1-deficient and wild-type hair bulbs revealed that expression of the diffusible factor *Kitl* (*Scf*) was also significantly downregulated in Notch1-deficient hair bulbs (Fig. 6C and see Table S1 in the supplementary material), suggesting that Notch1 is a positive regulator of this melanocyte survival factor in hair matrix cells. Indeed, multiple melanocyte signature transcripts were reduced (see Table S2 in the supplementary material) (Rendl et al., 2005), accompanied by a significant reduction in the number of melanocytes [identified by Dct immunohistochemistry] in Notch1-deficient hair bulbs (Fig. 6D,E), even after correcting for total keratinocyte numbers. Notch-mediated activation of Hes1 contributes autonomously to melanoblast survival (Moriyama et al., 2006); however, Hes1 expression was not compromised in the melanocytes of N1CKO skin (Fig. 8B and see Fig. S4 in the supplementary material). Therefore, *Kitl*-dependent proliferation and survival of follicular melanocytes (Botchkareva et al., 2001; Ito et al., 1999) is probably dependent on Notch1 activity in keratinocytes.

Differential impact of Notch1 loss on hair follicle and epidermal keratinocytes: underlying mechanisms?

In Notch1-deficient skin, the proliferation of epidermal keratinocytes increased progressively until a hyperplastic skin phenotype was evident, whereas follicular keratinocytes were hypoplastic, resulting in a shorter hair shaft (Fig. 1). To gain further insight into the basis of the differential response in these related keratinocyte populations, we compared the epidermal and follicular expression of selected Notch targets. The mRNA levels of *Nrarp* and *Heyl* (Krebs et al., 2001; Lamar et al., 2001) were reduced in the epidermis and in the hair follicle (Fig. 7C and Fig. 8A). Transcripts of these targets overlapped with Notch1 in the hair follicle (Fig. 8B). By contrast, epidermal Hes1 and p21^{Cip1} protein levels were reduced in Notch1-deficient epidermal keratinocytes (Fig. 7A,B), whereas their expression was unchanged in Notch1-deficient hair follicles (Fig. 3B and Fig. 8). Moreover, the location of expression of the Hes1 protein, a well-studied Notch target, did not overlap with that of *Notch1* mRNA (Fig. 8B) or protein (see Fig. S6 in the supplementary material). Instead, it overlapped with the expression domain of *Notch2* and *Notch3* (for details, see Pan et al., 2004). The expression domain of *Cdkn1a* mRNA overlapped with that of the Hes1 protein, supporting an indirect activation mechanism whereby Hes1 impacts the calcineurin (Ppp3ca)/nuclear factor of activated T-cells (NFAT) pathway (Mammucari et al., 2005). We conclude that p21^{Cip1} is probably a target of Hes1 (but not of Notch1) in both the epidermis and the hair follicle, and that Hes1 acts as a Notch1 target only in epidermal keratinocytes. In the hair follicle, its expression might be regulated by other Notch paralogs (Notch2 or Notch3). These data agree with a recent demonstration that vertebrate cellular context affects the usage of targets by individual Notch proteins in a manner yet to be explained (Cheng et al., 2007). These differences constitute a cell-autonomous contribution to the distinct proliferative behavior of hair follicles and epidermal keratinocytes in response to Notch1 loss.

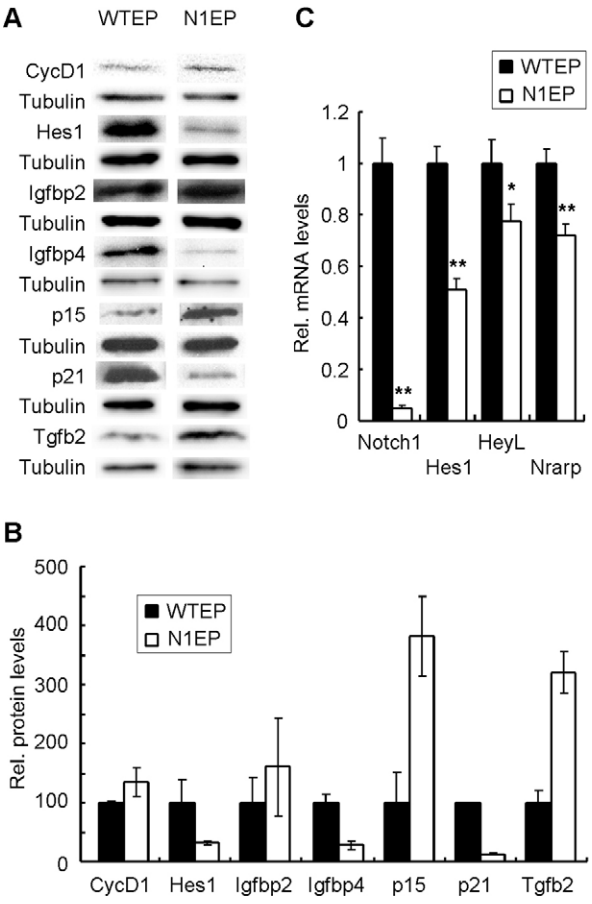

Fig. 7. Monitoring the epidermal expression of genes with altered expression in Notch1-deficient hair follicles. (**A**) Western blot analyses of postnatal day (P)9 epidermal cell lysates from embryo-deleted *Msx2-Cre;Notch1*$^{flox/flox}$ (N1CKO) mouse (N1EP) and its wild-type littermate (WTEP). (**B**) Quantification of the western data from A. (**C**) Quantitative reverse transcriptase (qRT)-PCR of *Notch1* and its targets, *Hes1*, *HeyL* and *Nrarp*, using P9 epidermal total RNA. Error bars represent s.e.m. **P*=0.05; ***P*<0.001.

DISCUSSION

Notch signaling has been shown to control the proliferation and differentiation of neighboring cells (Giraldez and Cohen, 2003; Lin and Kopan, 2003; Lin et al., 2000; Pan et al., 2004). Although several diffusible molecules, including Wingless and Unpaired, have been identified as mediators of such cell non-autonomous Notch functions in *Drosophila* (Giraldez and Cohen, 2003; Vaccari and Bilder, 2005), Kitl and Tgfβ are the first mammalian factors mediating bi-compartmental, Notch1-dependent signals that regulate proliferation or survival of a neighboring cell population (e.g. melanocytes within the hair follicles) to be identified. Nonetheless, reduced autocrine Kitl does not contribute to the Notch1-deficient follicular phenotypes, because animals treated with ACK2 (anti c-Kit antibody) or animals with mutations that reduced Kitl levels do not display any phenotypes reminiscent of Notch1 loss in their hair follicles (Besmer et al., 1993; Botchkareva et al., 2001; Lecoin et al., 1995; Okura et al., 1995). To our knowledge, this is also the first report to place Notch1 upstream of Tgfβ signaling in any cell type. Although, at this time, we can only speculate as to how Tgfβ ligands responded to Notch1 loss, the broad spectrum of co-regulated Tgfβ response genes confirm that this pathway is perturbed in response to Notch1 loss.

We observed a striking molecular difference between epidermis and hair follicles in the response of the stromal compartment to Tgfβ, specifically, in regulating the expression of Igfbp3 and Igfbp4. In Notch1-deficient hair follicles, induction of Igfbp3 underlies the

follicular phenotype in N1CKO animals. Overexpression of Igfbp4 can decrease the growth of prostate cancer (Durai et al., 2006); *Igfbp4* mRNA was also up regulated in the follicle (Fig. 5A) and might have also contributed to the downregulation of Igf1. By contrast, *Igfbp4* mRNA was significantly downregulated in Notch1-deficient dermis (Fig. 7A,B) (Batch et al., 1994). We thus posit that the differential modulation of IGF signaling as a consequence of changes in stromal IGFBP levels might underlie the difference in the response of epidermis and hair follicles to Notch1 loss. Therefore, the contribution of Notch signaling to differential follicular and epidermal homeostasis results from both cell-autonomous (differential target selection) and cell non-autonomous (differential stromal response to the same diffusible factors) effects, the latter mediated possibly by Tgfβ (Li et al., 2004; Liu et al., 2001).

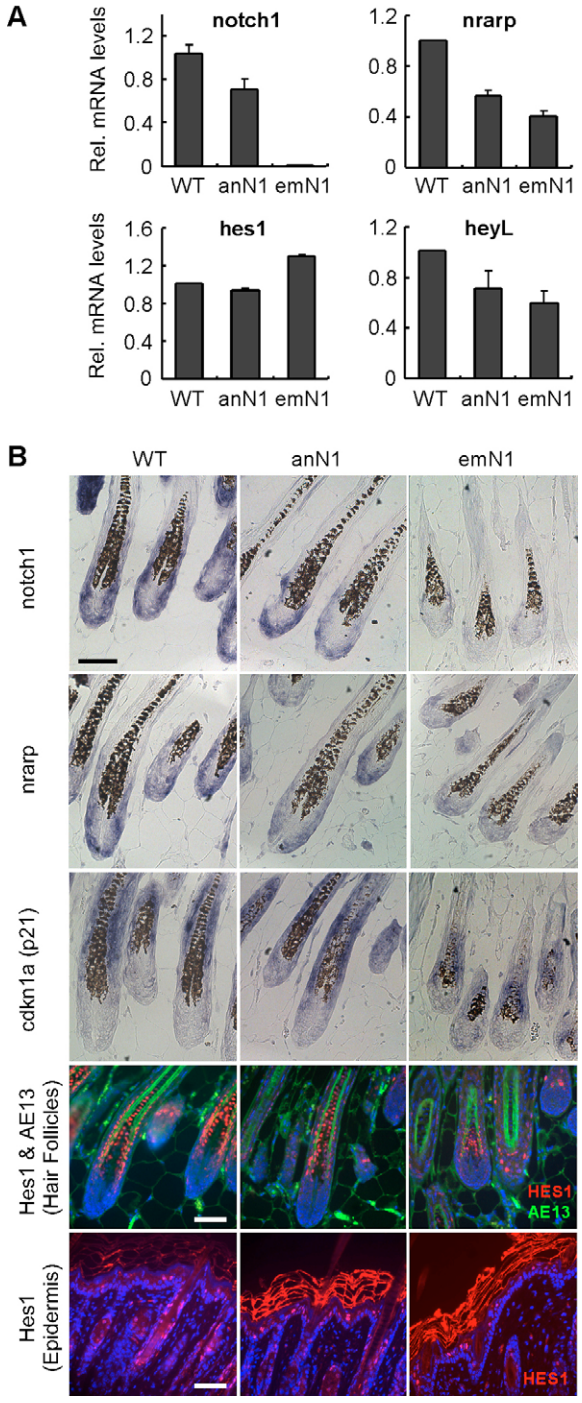

Fig. 8. Monitoring epidermal Notch targets for their expression in hair follicles. (**A**) Quantitative reverse transcriptase (qRT)-PCR for *Notch1*, *Nrarp*, *Hes1* and *Heyl*. Notice that *Hes1* expression was sustained in embryo-deleted Notch1 (em-N1) hair follicles. Error bars represent s.e.m. (**B**) mRNA (*Notch1*, *Nrarp* and *Cdkn1a*) and protein (Hes1) expression in skin. Hes1 (red) expression is found in differentiating hair matrix and epidermal suprabasal cells. AE13 (green) is a marker for follicular cortex and cuticle. Nuclei were stained with DAPI. anN1, anagen-deleted Notch1; WT, wild type. Scale bars: 40 μm.

Non-autonomous components of hair cycling revealed in chimeric skin

Entry into catagen was accelerated in 90% of follicles when Notch1 was removed throughout the entire skin surface [*K14-Cre and K5-Cre^{ERT}* (Vauclair et al., 2005)]. However, catagen was not accelerated in N1CKO mice, in which Notch1-deficient hair follicles resided in a heterogeneous environment (i.e. in the presence of anN1 follicles, which have a wild-type phenotype). Instead, synchronicity is maintained in the chimeric skin, with Notch1-deficient follicles entering catagen along with the anN1 follicles. Our studies provide mechanistic insight into the role of Notch1 in catagen induction.

Although several pro-catagen transcripts were elevated when Notch1 was lost, these changes were not sufficient to permit catagen onset in our chimeric N1CKO mice. For example, detection of *Igfbp3* mRNA in N1CKO skin by in situ hybridization (ISH) required an extended incubation time in NBT reagent (48 hours) compared with signal development in early catagen follicles (3 hours; see Fig. S5 in the supplementary material). If catagen onset relied only on follicle-intrinsic mechanisms, it would be expected that Notch1-deficient follicles would enter catagen early, even if embedded in a heterogeneous environment. It is important to consider that, although our mice had chimeric skin, most individual follicles were not salt-and-paper mosaics; they either expressed *Notch1* or they did not (Fig. 1A, Fig. 8B and see Fig. S6 in the supplementary material). This implies that the milder phenotype we see in Notch1-deficient follicles is not simply due to rescue by wild-type matrix cells.

Several other possible explanations for this observation exist. First, the timing of Notch1 deletion in these experimental paradigms differs: dorsal ectodermal *Msx2-Cre* expression (Pan et al., 2004) precedes dorsal keratin 14 (*K14*) expression (Byrne et al., 1994); the earliest catagen was induced by the postnatal Cre-mediated deletion [by *K5-Cre^{ERT}* in newborn mice (Vauclair et al., 2005)]. Perhaps early deletion allowed for compensation by an intrinsic follicular factor. Alternatively, accelerated catagen might be due, in part, to Cre-mediated toxicity (Loonstra et al., 2001; Schmidt et al., 2000), which might be more severe with postnatal Cre induction. However, we cannot rule out a third possibility: that the presence of wild-type epidermis and follicles in *Msx2-Cre* lines ameliorates the impact of Notch1 loss by the generation of systemic, diffusible factor(s) that can entrain the cycling of Notch1-deficient follicles (Stenn and Paus, 2001) and prevent them from entering into catagen.

In conclusion, the response of wild-type stromal cells to signals produced by mutant epithelial neighbors crucially contributes to cancer (Krtolica and Campisi, 2002; Krtolica and Campisi, 2003). We demonstrate that Notch1 contributes to an elaborate network of signaling pathways that monitor and control proliferation in the skin. The effects of Notch1 loss in the skin are reminiscent of the transformation of cells adjacent to Notch-deficient clones in *Drosophila* (Moberg et al., 2005; Thompson et al., 2005; Vaccari

and Bilder, 2005). Our observations suggest that the skin tumorigenesis resulting from Notch loss is in part mediated by elevation in the level of ligands that elicit stromal responses, similar to the 'vicious cycle' that promotes bone metastasis in several solid cancers (Mundy, 2002; Roodman, 2004). In a broader context, the role of Notch signaling in tumor suppression might reflect both an autonomous function in promoting keratinocyte differentiation and a non-autonomous function within a signaling network that regulates keratinocyte proliferation.

The authors wish to thank Anne Bowcock, Tatiana Efimova, Jeffrey Gordon, Meei-hua Lin, Liang Ma and the members of the Kopan laboratory for careful reading and numerous consultations throughout the course of this work. We are grateful for Maxene Ilagan's critical reading of the manuscript. We wish to thank Gail Martin and Thomas Schlake for the *Msx2-Cre* and *Ivl::Igf1* mice, respectively. J.L. and R.K. were supported in part by Washington University and by grants from the NIH-NIGMS (GM55479-10) and NIHD (HD044056-01).

Supplementary material

Supplementary material for this article is available at
http://dev.biologists.org/cgi/content/full/134/15/2795/DC1

References

Alonso, L. and Fuchs, E. (2003). Stem cells in the skin: waste not, Wnt not. *Genes Dev.* **17**, 1189-1200.
Bartek, J. and Lukas, J. (2001). Mammalian G1- and S-phase checkpoints in response to DNA damage. *Curr. Opin. Cell Biol.* **13**, 738-747.
Baserga, R., Hongo, A., Rubini, M., Prisco, M. and Valentinis, B. (1997). The IGF-I receptor in cell growth, transformation and apoptosis. *Biochim. Biophys. Acta* **1332**, F105-F126.
Batch, J. A., Mercuri, F. A., Edmondson, S. R. and Werther, G. A. (1994). Localization of messenger ribonucleic acid for insulin-like growth factor-binding proteins in human skin by in situ hybridization. *J. Clin. Endocrinol. Metab.* **79**, 1444-1449.
Besmer, P., Manova, K., Duttlinger, R., Huang, E. J., Packer, A., Gyssler, C. and Bachvarova, R. F. (1993). The kit-ligand (steel factor) and its receptor c-kit/W: pleiotropic roles in gametogenesis and melanogenesis. *Dev. Suppl.* **1993**, 125-137.
Blanpain, C., Lowry, W. E., Pasolli, H. A. and Fuchs, E. (2006). Canonical notch signaling functions as a commitment switch in the epidermal lineage. *Genes Dev.* **20**, 3022-3035.
Botchkareva, N. V., Khlgatian, M., Longley, B. J., Botchkarev, V. A. and Gilchrest, B. A. (2001). SCF/c-kit signaling is required for cyclic regeneration of the hair pigmentation unit. *FASEB J.* **15**, 645-658.
Brown, C. B., Boyer, A. S., Runyan, R. B. and Barnett, J. V. (1999). Requirement of type III TGF-beta receptor for endocardial cell transformation in the heart. *Science* **283**, 2080-2082.
Butt, A. J., Firth, S. M. and Baxter, R. C. (1999). The IGF axis and programmed cell death. *Immunol. Cell Biol.* **77**, 256-262.
Byrne, C., Tainsky, M. and Fuchs, E. (1994). Programming gene expression in developing epidermis. *Development* **120**, 2369-2383.
Cheng, H. T., Kim, M., Valerius, M. T., Surendran, K., Schuster-Gossler, K., Gossler, A., McMahon, A. P. and Kopan, R. (2007). Notch2, but not Notch1, is required for proximal fate acquisition in the mammalian nephron. *Development* **134**, 801-811.
Chenn, A. and Walsh, C. A. (2002). Regulation of cerebral cortical size by control of cell cycle exit in neural precursors. *Science* **297**, 365-369.
Clayton, E., Doupe, D. P., Klein, A. M., Winton, D. J., Simons, B. D. and Jones, P. H. (2007). A single type of progenitor cell maintains normal epidermis. *Nature* **446**, 185-189.
Cui, W., Fowlis, D. J., Cousins, F. M., Duffie, E., Bryson, S., Balmain, A. and Akhurst, R. J. (1995). Concerted action of TGF-beta 1 and its type II receptor in control of epidermal homeostasis in transgenic mice. *Genes Dev.* **9**, 945-955.
Devgan, V., Mammucari, C., Millar, S. E., Brisken, C. and Dotto, G. P. (2005). p21WAF1/Cip1 is a negative transcriptional regulator of Wnt4 expression downstream of Notch1 activation. *Genes Dev.* **19**, 1485-1495.
DiSalvo, C. V., Zhang, D. and Jacobberger, J. W. (1995). Regulation of NIH-3T3 cell G1 phase transit by serum during exponential growth. *Cell Prolif.* **28**, 511-524.
Dry, F. W. (1926). The coat of the mouse (*Mus musculus*). *J. Genet.* **16**, 287-340.
Durai, R., Davies, M., Yang, W., Yang, S. Y., Seifalian, A., Goldspink, G. and Winslet, M. (2006). Biology of insulin-like growth factor binding protein-4 and its role in cancer (review). *Int. J. Oncol.* **28**, 1317-1325.
Edmondson, S. R., Thumiger, S. P., Werther, G. A. and Wraight, C. J. (2003). Epidermal homeostasis: the role of the growth hormone and insulin-like growth factor systems. *Endocr. Rev.* **24**, 737-764.
Firth, S. M. and Baxter, R. C. (2002). Cellular actions of the insulin-like growth factor binding proteins. *Endocr. Rev.* **23**, 824-854.
Fryer, C. J., White, J. B. and Jones, K. A. (2004). Mastermind recruits CycC:CDK8 to phosphorylate the notch ICD and coordinate activation with turnover. *Mol. Cell* **16**, 509-520.
Fuchs, E. and Raghavan, S. (2002). Getting under the skin of epidermal morphogenesis. *Nat. Rev. Genet.* **3**, 199-209.
Giraldez, A. J. and Cohen, S. M. (2003). Wingless and Notch signaling provide cell survival cues and control cell proliferation during wing development. *Development* **130**, 6533-6543.
Guo, Y. S., Townsend, C. M., Jr, Jin, G. F., Beauchamp, R. D. and Thompson, J. C. (1995). Differential regulation by TGF-beta 1 and insulin of insulin-like growth factor binding protein-2 in IEC-6 cells. *Am. J. Physiol. Endocrinol. Metab.* **268**, E1199-E1204.
Hardy, M. H. (1992). The secret life of the hair follicle. *Trends Genet.* **8**, 55-61.
Harms, K. L. and Chen, X. (2005). The C terminus of p53 family proteins is a cell fate determinant. *Mol. Cell. Biol.* **25**, 2014-2030.
Huang, Q., Raya, A., DeJesus, P., Chao, S. H., Quon, K. C., Caldwell, J. S., Chanda, S. K., Izpisua-Belmonte, J. C. and Schultz, P. G. (2004). Identification of p53 regulators by genome-wide functional analysis. *Proc. Natl. Acad. Sci. USA* **101**, 3456-3461.
Inagaki, Y., Truter, S. and Ramirez, F. (1994). Transforming growth factor-beta stimulates alpha 2(I) collagen gene expression through a cis-acting element that contains an Sp1-binding site. *J. Biol. Chem.* **269**, 14828-14834.
Ito, M., Kawa, Y., Ono, H., Okura, M., Baba, T., Kubota, Y., Nishikawa, S. I. and Mizoguchi, M. (1999). Removal of stem cell factor or addition of monoclonal anti-c-KIT antibody induces apoptosis in murine melanocyte precursors. *J. Invest. Dermatol.* **112**, 796-801.
Ito, M., Liu, Y., Yang, Z., Nguyen, J., Liang, F., Morris, R. J. and Cotsarelis, G. (2005). Stem cells in the hair follicle bulge contribute to wound repair but not to homeostasis of the epidermis. *Nat. Med.* **11**, 1351-1354.
Ito, T., Udaka, N., Yazawa, T., Okudela, K., Hayashi, H., Sudo, T., Guillemot, F., Kageyama, R. and Kitamura, H. (2000). Basic helix-loop-helix transcription factors regulate the neuroendocrine differentiation of fetal mouse pulmonary epithelium. *Development* **127**, 3913-3921.
Jacks, T., Remington, L., Williams, B. O., Schmitt, E. M., Halachmi, S., Bronson, R. T. and Weinberg, R. A. (1994). Tumor spectrum analysis in p53-mutant mice. *Curr. Biol.* **4**, 1-7.
Jamora, C. and Fuchs, E. (2002). Intercellular adhesion, signalling and the cytoskeleton. *Nat. Cell Biol.* **4**, E101-E108.
Jetten, A. M., Shirley, J. E. and Stoner, G. (1986). Regulation of proliferation and differentiation of respiratory tract epithelial cells by TGF beta. *Exp. Cell Res.* **167**, 539-549.
Kopan, R. (2002). Notch: a membrane-bound transcription factor. *J. Cell Sci.* **115**, 1095-1097.
Kopan, R. and Weintraub, H. (1993). Mouse notch: expression in hair follicles correlates with cell fate determination. *J. Cell Biol.* **121**, 631-641.
Krebs, L. T., Deftos, M. L., Bevan, M. J. and Gridley, T. (2001). The Nrarp gene encodes an ankyrin-repeat protein that is transcriptionally regulated by the Notch signaling pathway. *Dev. Biol.* **238**, 110-119.
Krtolica, A. and Campisi, J. (2002). Cancer and aging: a model for the cancer promoting effects of the aging stroma. *Int. J. Biochem. Cell Biol.* **34**, 1401-1414.
Krtolica, A. and Campisi, J. (2003). Integrating epithelial cancer, aging stroma and cellular senescence. *Adv. Gerontol.* **11**, 109-116.
Lamar, E., Deblandre, G., Wettstein, D., Gawantka, V., Pollet, N., Niehrs, C. and Kintner, C. (2001). Nrarp is a novel intracellular component of the Notch signaling pathway. *Genes Dev.* **15**, 1885-1899.
Lechler, T. and Fuchs, E. (2005). Asymmetric cell divisions promote stratification and differentiation of mammalian skin. *Nature* **437**, 275-280.
Lecoin, L., Lahav, R., Martin, F. H., Teillet, M. A. and Le Douarin, N. M. (1995). Steel and c-kit in the development of avian melanocytes: a study of normally pigmented birds and of the hyperpigmented mutant silky fowl. *Dev. Dyn.* **203**, 106-118.
Legue, E. and Nicolas, J. F. (2005). Hair follicle renewal: organization of stem cells in the matrix and the role of stereotyped lineages and behaviors. *Development* **132**, 4143-4154.
Li, A. G., Wang, D., Feng, X. H. and Wang, X. J. (2004). Latent TGFbeta1 overexpression in keratinocytes results in a severe psoriasis-like skin disorder. *EMBO J.* **23**, 1770-1781.
Lin, M. H. and Kopan, R. (2003). Long-range, nonautonomous effects of activated Notch1 on tissue homeostasis in the nail. *Dev. Biol.* **263**, 343-359.
Lin, M. H., Leimeister, C., Gessler, M. and Kopan, R. (2000). Activation of the Notch pathway in the hair cortex leads to aberrant differentiation of the adjacent hair-shaft layers. *Development* **127**, 2421-2432.
Lindner, G., Botchkarev, V., Botchkareva, N., Ling, G., van der Veen, C. and Paus, R. (1997). Analysis of apoptosis during hair follicle regression (catagen). *Am. J. Pathol.* **151**, 1601-1617.
Liu, X., Alexander, V., Vijayachandra, K., Bhogte, E., Diamond, I. and Glick, A. (2001). Conditional epidermal expression of TGFbeta 1 blocks neonatal

lethality but causes a reversible hyperplasia and alopecia. *Proc. Natl. Acad. Sci. USA* **98**, 9139-9144.
Loonstra, A., Vooijs, M., Beverloo, H. B., Allak, B. A., van Drunen, E., Kanaar, R., Berns, A. and Jonkers, J. (2001). Growth inhibition and DNA damage induced by Cre recombinase in mammalian cells. *Proc. Natl. Acad. Sci. USA* **98**, 9209-9214.
Lunny, D. P., Weed, E., Nolan, P. M., Marquardt, A., Augustin, M. and Porter, R. M. (2005). Mutations in gasdermin 3 cause aberrant differentiation of the hair follicle and sebaceous gland. *J. Invest. Dermatol.* **124**, 615-621.
Mainprize, T. G., Taylor, M. D., Rutka, J. T. and Dirks, P. B. (2001). Cip/Kip cell-cycle inhibitors: a neuro-oncological perspective. *J. Neuro-oncol.* **51**, 205-218.
Malkinson, F. D. and Keane, J. T. (1978). Hair matrix cell kinetics: a selective review. *Int. J. Dermatol.* **17**, 536-551.
Mammucari, C., di Vignano, A. T., Sharov, A. A., Neilson, J., Havrda, M. C., Roop, D. R., Botchkarev, V. A., Crabtree, G. R. and Dotto, G. P. (2005). Integration of Notch 1 and calcineurin/NFAT signaling pathways in keratinocyte growth and differentiation control. *Dev. Cell* **8**, 665-676.
Martin, J. L. and Baxter, R. C. (1991). Transforming growth factor-beta stimulates production of insulin-like growth factor-binding protein-3 by human skin fibroblasts. *Endocrinology* **128**, 1425-1433.
Massague, J. (2004). G1 cell-cycle control and cancer. *Nature* **432**, 298-306.
Millar, S. E. (2002). Molecular mechanisms regulating hair follicle development. *J. Invest. Dermatol.* **118**, 216-225.
Moberg, K. H., Schelble, S., Burdick, S. K. and Hariharan, I. K. (2005). Mutations in erupted, the Drosophila ortholog of mammalian tumor susceptibility gene 101, elicit non-cell-autonomous overgrowth. *Dev. Cell* **9**, 699-710.
Moll, U. M. and Slade, N. (2004). p63 and p73: roles in development and tumor formation. *Mol. Cancer Res.* **2**, 371-386.
Moriyama, M., Osawa, M., Mak, S.-S., Ohtsuka, T., Yamamoto, N., Han, H., Delmas, V., Kageyama, R., Beermann, F., Larue, L. et al. (2006). Notch signaling via Hes1 transcription factor maintains survival of melanoblasts and melanocyte stem cells. *J. Cell Biol.* **173**, 333-339.
Moustakas, A., Pardali, K., Gaal, A. and Heldin, C. H. (2002). Mechanisms of TGF-beta signaling in regulation of cell growth and differentiation. *Immunol. Lett.* **82**, 85-91.
Muller-Rover, S., Handjiski, B., van der Veen, C., Eichmuller, S., Foitzik, K., McKay, I. A., Stenn, K. S. and Paus, R. (2001). A comprehensive guide for the accurate classification of murine hair follicles in distinct hair cycle stages. *J. Invest. Dermatol.* **117**, 3-15.
Mumm, J. S. and Kopan, R. (2000). Notch signaling: from the outside in. *Dev. Biol.* **228**, 151-165.
Mundy, G. R. (2002). Metastasis to bone: causes, consequences and therapeutic opportunities. *Nat. Rev. Cancer* **2**, 584-593.
Nguyen, B.-C., Lefort, K., Mandinova, A., Antonini, D., Devgan, V., Della Gatta, G., Koster, M. I., Zhang, Z., Wang, J., di Vignano, A. T. et al. (2006). Cross-regulation between Notch and p63 in keratinocyte commitment to differentiation. *Genes Dev.* **20**, 1028-1042.
Nicolas, M., Wolfer, A., Raj, K., Kummer, J. A., Mill, P., van Noort, M., Hui, C. C., Clevers, H., Dotto, G. P. and Radtke, F. (2003). Notch1 functions as a tumor suppressor in mouse skin. *Nat. Genet.* **33**, 416-421.
Okura, M., Maeda, H., Nishikawa, S. and Mizoguchi, M. (1995). Effects of monoclonal anti-c-kit antibody (ACK2) on melanocytes in newborn mice. *J. Invest. Dermatol.* **105**, 322-328.
Okuyama, R., Nguyen, B. C., Talora, C., Ogawa, E., Tommasi di Vignano, A., Lioumi, M., Chiorino, G., Tagami, H., Woo, M. and Dotto, G. P. (2004). High commitment of embryonic keratinocytes to terminal differentiation through a Notch1-caspase 3 regulatory mechanism. *Dev. Cell* **6**, 551-562.
Pan, Y., Lin, M.-H., Tian, X., Cheng, H.-T., Gridley, T., Shen, J. and Kopan, R. (2004). γ-Secretase functions through notch signaling to maintain skin appendages but is not required for their patterning or initial morphogenesis. *Dev. Cell* **7**, 731-743.
Paus, R., Foitzik, K., Welker, P., Bulfone-Paus, S. and Eichmuller, S. (1997). Transforming growth factor-beta receptor type I and type II expression during murine hair follicle development and cycling. *J. Invest. Dermatol.* **109**, 518-526.
Rangarajan, A., Talora, C., Okuyama, R., Nicolas, M., Mammucari, C., Oh, H., Aster, J. C., Krishna, S., Metzger, D., Chambon, P. et al. (2001). Notch signaling is a direct determinant of keratinocyte growth arrest and entry into differentiation. *EMBO J.* **20**, 3427-3436.
Rendl, M., Lewis, L. and Fuchs, E. (2005). Molecular dissection of mesenchymal-epithelial interactions in the hair follicle. *PLoS Biol.* **3**, e331.
Resnicoff, M. and Baserga, R. (1998). The role of the insulin-like growth factor I receptor in transformation and apoptosis. *Ann. N. Y. Acad. Sci.* **842**, 76-81.
Roodman, G. D. (2004). Mechanisms of bone metastasis. *N. Engl. J. Med.* **350**, 1655-1664.
Rossi, M., Sayan, A. E., Terrinoni, A., Melino, G. and Knight, R. A. (2004). Mechanism of induction of apoptosis by p73 and its relevance to neuroblastoma biology. *Ann. N. Y. Acad. Sci.* **1028**, 143-149.
Saeki, N., Kuwahara, Y., Sasaki, H., Satoh, H. and Shiroishi, T. (2000). Gasdermin (Gsdm) localizing to mouse Chromosome 11 is predominantly expressed in upper gastrointestinal tract but significantly suppressed in human gastric cancer cells. *Mamm. Genome* **11**, 718-724.
Scandura, J. M., Boccuni, P., Massague, J. and Nimer, S. D. (2004). Transforming growth factor {beta}-induced cell cycle arrest of human hematopoietic cells requires p57KIP2 up-regulation. *Proc. Natl. Acad. Sci. USA* **101**, 15231-15236.
Schmidt, E. E., Taylor, D. S., Prigge, J. R., Barnett, S. and Capecchi, M. R. (2000). Illegitimate Cre-dependent chromosome rearrangements in transgenic mouse spermatids. *Proc. Natl. Acad. Sci. USA* **97**, 13702-13707.
Sengel, P. (1976). *Morphogenesis of Skin*. Cambridge: Cambridge University Press.
Sherr, C. J. and Roberts, J. M. (1999). CDK inhibitors: positive and negative regulators of G1-phase progression. *Genes Dev.* **13**, 1501-1512.
Stenn, K. S. and Paus, R. (2001). Controls of hair follicle cycling. *Physiol. Rev.* **81**, 449-494.
Su, H. Y., Hickford, J. G., Bickerstaffe, R. and Palmer, B. R. (1999a). Insulin-like growth factor 1 and hair growth. *Dermatol. Online J.* **5**, 1.
Su, H. Y., Hickford, J. G., The, P. H., Hill, A. M., Frampton, C. M. and Bickerstaffe, R. (1999b). Increased vibrissa growth in transgenic mice expressing insulin-like growth factor 1. *J. Invest. Dermatol.* **112**, 245-248.
Sun, X., Lewandoski, M., Meyers, E. N., Liu, Y. H., Maxson, R. E., Jr and Martin, G. R. (2000). Conditional inactivation of Fgf4 reveals complexity of signalling during limb bud development. *Nat. Genet.* **25**, 83-86.
Terrinoni, A., Ranalli, M., Cadot, B., Leta, A., Bagetta, G., Vousden, K. H. and Melino, G. (2004). p73-alpha is capable of inducing scotin and ER stress. *Oncogene* **23**, 3721-3725.
Thompson, B. J., Mathieu, J., Sung, H. H., Loeser, E., Rorth, P. and Cohen, S. M. (2005). Tumor suppressor properties of the ESCRT-II complex component Vps25 in Drosophila. *Dev. Cell* **9**, 711-720.
Vaccari, T. and Bilder, D. (2005). The Drosophila tumor suppressor vps25 prevents nonautonomous overproliferation by regulating notch trafficking. *Dev. Cell* **9**, 687-698.
Vauclair, S., Nicolas, M., Barrandon, Y. and Radtke, F. (2005). Notch1 is essential for postnatal hair follicle development and homeostasis. *Dev. Biol*. **284**, 184-193.
Weedon, D. and Strutton, G. (1981). Apoptosis as the mechanism of the involution of hair follicles in catagen transformation. *Acta Derm. Venereol.* **61**, 335-339.
Weger, N. and Schlake, T. (2005a). IGF-I signalling controls the hair growth cycle and the differentiation of hair shafts. *J. Invest. Dermatol.* **125**, 873-882.
Weger, N. and Schlake, T. (2005b). Igfbp3 modulates cell proliferation in the hair follicle. *J. Invest. Dermatol.* **125**, 847-849.
Yamamoto, N., Tanigaki, K., Han, H., Hiai, H. and Honjo, T. (2003). Notch/RBP-J Signaling regulates epidermis/hair fate determination of hair follicular stem cells. *Curr. Biol.* **13**, 333-338.
Yang, X., Klein, R., Tian, X., Cheng, H. T., Kopan, R. and Shen, J. (2004). Notch activation induces apoptosis in neural progenitor cells through a p53-dependent pathway. *Dev. Biol.* **269**, 81-94.
Zheng, B., Zhang, Z., Black, C. M., de Crombrugghe, B. and Denton, C. P. (2002). Ligand-dependent genetic recombination in fibroblasts: a potentially powerful technique for investigating gene function in fibrosis. *Am. J. Pathol.* **160**, 1609-1617.

Table S1. Genes with altered expression in Notch1-deficient proximal hair bulbs classified under the GO categories of cell growth, cycle, proliferation and programmed cell death

Probe set ID	Gene symbol	Gene title	emN1 vs anN1 (1)	emN1 vs anN1 (2)	qRT-PCR validation
Cell cycle/growth/proliferation					
1456022_at	*B230339E18Rik*	RIKEN cDNA B230339E18 gene	–2.32	–1.74	
1418971_x_at	*Bcl10*	B-cell leukemia/lymphoma 10	1.56	1.62	
1418970_a_at	*Bcl10*	B-cell leukemia/lymphoma 10	1.62	1.62	
1422477_at	*Cables1*	Cdk5 and Abl enzyme substrate 1	2.5	1.63	
1441938_x_at	*Cables1*	Cdk5 and Abl enzyme substrate 1	2.01	1.92	
1455869_at	*Camk2b*	Calcium/calmodulin-dependent protein kinase II, beta	2.56	2.3	
1449145_a_at	*Cav1*	caveolin, caveolae protein 1	2.98	3.23	
1417327_at	*Cav2*	caveolin 2	3.31	2.29	
1417419_at	*Ccnd1*	cyclin D1	–2.37	–2.32	NC
1448698_at	*Ccnd1*	cyclin D1	–1.5	–1.79	NC
1417649_at	*Cdkn1c*	cyclin-dependent kinase inhibitor 1C (P57)	2.43	2.22	√
1449152_at	*Cdkn2b*	cyclin-dependent kinase inhibitor 2B (p15, inhibits CDK4)	1.72	1.83	√
1450944_at	*Cspg4*	chondroitin sulfate proteoglycan 4	3.53	1.94	
1423341_at	*Cspg4*	chondroitin sulfate proteoglycan 4	4.9	3.12	
1448823_at	*Cxcl12*	chemokine (C-X-C motif) ligand 12	6.22	4.19	
1421117_at	*Dst*	dystonin	2.96	2.39	
1419431_at	*Ereg*	epiregulin	2.87	2.88	
1416268_at	*Ets2*	E26 avian leukemia oncogene 2, 3′ domain	1.78	1.78	
1438883_at	*Fgf5*	fibroblast growth factor 5	–1.56	–2.57	
1416855_at	*Gas1*	growth arrest specific 1	2.3	2.78	
1417399_at	*Gas6*	growth arrest specific 6	2.52	2.1	
1459211_at	*Gli2*	GLI-Kruppel family member GLI2	1.58	1.6	
1446086_s_at	*Gli2*	GLI-Kruppel family member GLI2	2.08	1.61	
1419292_at	*Htra3*	serine protease HTRA3	2.33	4.63	
1454159_a_at	*Igfbp2*	insulin-like growth factor binding protein 2	5.8	7.05	√
1458268_s_at	*Igfbp3*	insulin-like growth factor binding protein 3	8.03	4.05	√
1423062_at	*Igfbp3*	insulin-like growth factor binding protein 3	6.4	5.98	√
1437406_x_at	*Igfbp4*	insulin-like growth factor binding protein 4	1.51	1.75	√
1423757_x_at	*Igfbp4*	insulin-like growth factor binding protein 4	1.74	1.85	√
1423756_s_at	*Igfbp4*	insulin-like growth factor binding protein 4	1.89	1.89	√
1423584_at	*Igfbp7*	insulin-like growth factor binding protein 7	2.58	1.96	
1421066_at	*Jak2*	Janus kinase 2	1.63	1.51	
1421317_x_at	*Myb*	myeloblastosis oncogene	1.86	2.37	
1450194_a_at	*Myb*	myeloblastosis oncogene	2.22	2.56	
1422818_at	*Nedd9*	neural precursor cell expressed, developmentally down-regulated gene 9	2.09	1.53	
1438157_s_at	*Nfkbia*	nuclear factor of kappa light chain gene enhancer in B-cells inhibitor, alpha	1.5	1.8	
1448306_at	*Nfkbia*	nuclear factor of kappa light chain gene enhancer in B-cells inhibitor, alpha	1.89	2.25	
1421917_at	*Pdgfra*	platelet derived growth factor receptor, alpha polypeptide	1.56	1.84	
1417133_at	*Pmp22*	peripheral myelin protein	2.11	1.99	
1438251_x_at	*Prss11*	protease, serine, 11 (Igf binding)	2.29	2.35	
1416749_at	*Prss11*	protease, serine, 11 (Igf binding)	2.47	2.55	
1447830_s_at	*Rgs2*	regulator of G-protein signaling 2	5.19	3.54	
1419248_at	*Rgs2*	regulator of G-protein signaling 2	6.32	3.63	
1419247_at	*Rgs2*	regulator of G-protein signaling 2	5.96	3.84	
1418448_at	*Rras*	Harvey rat sarcoma oncogene, subgroup R	2.1	1.95	
1456212_x_at	*Socs3*	suppressor of cytokine signaling 3	6.63	2.13	
1455899_x_at	*Socs3*	suppressor of cytokine signaling 3	2.73	2.21	
1421943_at	*Tgfa*	transforming growth factor alpha	4.31	3.28	
1423250_a_at	*Tgfb2*	transforming growth factor, beta 2	3.45	1.83	√
1450923_at	*Tgfb2*	transforming growth factor, beta 2	3.36	2.23	√
1450922_a_at	*Tgfb2*	transforming growth factor, beta 2	3.15	2.86	√
1426397_at	*Tgfbr2*	transforming growth factor, beta receptor II	2.23	2.16	√
1460302_at	*Thbs1*	Thrombospondin 1	3.46	3.06	

Programmed cell death					
1456022_at	*B230339E18Rik*	RIKEN cDNA B230339E18 gene	–2.32	–1.74	
1418971_x_at	*Bcl10*	B-cell leukemia/lymphoma 10	1.56	1.62	
1418970_a_at	*Bcl10*	B-cell leukemia/lymphoma 10	1.62	1.62	
1421392_a_at	*Birc3*	baculoviral IAP repeat-containing 3	2.17	1.77	
1454880_s_at	*Bmf*	Bcl2 modifying factor	1.9	1.69	
1417040_a_at	*Bok*	Bcl-2-related ovarian killer protein	1.57	1.71	
1416855_at	*Gas1*	growth arrest specific 1	2.3	2.78	
1435040_at	*Irak3*	interleukin-1 receptor-associated kinase 3	2.56	2.79	
1421066_at	*Jak2*	Janus kinase 2	1.63	1.51	
1420640_at	*Jmy*	junction-mediating and regulatory protein	1.53	1.66	
1454974_at	*Ntn1*	netrin 1	4.22	2.89	
1423986_a_at	*Scotin*	scotin gene	1.91	1.73	√
1450036_at	*Sgk3*	serum/glucocorticoid regulated kinase 3	2.11	1.62	
1418011_a_at	*Sh3glb1*	SH3-domain GRB2-like B1 (endophilin)	1.66	1.56	
1433699_at	*Tnfaip3*	tumor necrosis factor, alpha-induced protein 3	1.71	1.59	
1416926_at	*Trp53inp1*	transformation related protein 53 inducible nuclear protein 1	1.81	1.72	
1452325_at	*Trp73*	transformation related protein 73	4.19	3.28	√
Others					
1460302_at	*Thbs1*	thrombospondin 1	4.2	3.65	
1421811_at	*Thbs1*	thrombospondin 1	3.64	5.04	
1415855_at	*Kitl*	Kit ligand	–3.24	–2.63	√

A total of 622 genes differentially regulated in Notch1-deficient proximal bulbs were classified by gene ontology (GO) terms. emN1 vs anN1 (1)/emN1 vs anN1 (2), indicate two different microarray experiments. Validated genes by qRT-PCR were marked as √ and the genes with no significant change as NC.

Table S2. Altered expression of melanocyte signature genes in Notch1-deficient hair bulbs

Probe set ID	Gene symbol	Gene title	emN1 vs anN1 (1)	emN1 vs anN1 (2)
1423989_at	*2210010N04Rik*	RIKEN cDNA 2210010N04 gene	–1.78	–3.8
1434175_s_at	*2210010N04Rik*	RIKEN cDNA 2210010N04 gene	–2.12	–2.25
1416607_at	*4931406C07Rik*	RIKEN cDNA 4931406C07 gene	–2.52	–1.99
1433671_at	*A130022J15Rik*	RIKEN cDNA A130022J15 gene	–1.7	–1.89
1454678_s_at	*A130022J15Rik*	RIKEN cDNA A130022J15 gene	–1.58	–1.82
1450380_at	*AU040950*	ependymin 2	–3.54	–3.49
1435758_at	*B4galt6*	UDP-Gal:betaGlcNAc beta 1,4-galactosyltransferase, polypeptide6	–1.68	–1.75
1416673_at	*Bace2*	beta-site APP-cleaving enzyme 2	–2.19	–3.34
1424383_at	*BC003277*	cDNA sequence BC003277	–1.87	–1.71
1418476_at	*Crlf1*	cytokine receptor-like factor 1	–3.46	–3.63
1418365_at	*Ctsh*	cathepsin H	3.08	2.63
1450779_at	*Fabp7*	fatty acid binding protein 7, brain	–4.48	–3.55
1420581_at	*Gpr143*	mouse homolog of human ocular albinism 1 (Nettleship-Falls)	–5.11	–4.18
1421040_a_at	*Gsta2*	glutathione S-transferase, alpha 2 (Yc2)	–7.07	–5.76
1451055_at	*Matp*	membrane associated transporter protein	–3.71	–4.00
1437430_at	*Matp*	membrane associated transporter protein	–2.82	–3.27
1437540_at	*Mcoln3*	mucolipin 3	–2.99	–2.97
1450391_a_at	*Mgll*	monoglyceride lipase	–1.73	–1.82
1449896_at	*Mlph*	melanophilin	–2.1	–2.02
1419127_at	*Npy*	neuropeptide Y	–2.21	–2.51
1426588_at	*Ocsp*	oculospanin	–3.09	–3.11
1418211_at	*P*	pink-eyed dilution	–3.52	–4.09
1418835_at	*Phlda1*	pleckstrin homology-like domain, family A, member 1	–1.5	–1.53
1423213_at	*Plxnc1*	plexin C1	–3.17	–3.42
1450905_at	*Plxnc1*	plexin C1	–3.19	–2.52
1423860_at	*Ptgds*	prostaglandin D2 synthase (brain)	–2.63	–2.83
1423859_a_at	*Ptgds*	prostaglandin D2 synthase (brain)	–2.65	–2.07
1416527_at	*Rab32*	RAB32, member RAS oncogene family	–1.85	–1.75
1417700_at	*Rab38*	Rab38, member of RAS oncogene family	–2.94	–3.35
1448595_a_at	*Rex3*	reduced expression 3	3.79	4.5
1449078_at	*Siat10*	sialyltransferase 10 (alpha-2,3-sialyltransferase VI)	–3.32	–3.18
1418326_at	*Slc7a5*	solute carrier family 7 (cationic amino acid transporter, y+ system), member 5	–1.61	–2.85
1451689_a_at	*Sox10*	SRY-box containing gene 10	–3.12	–3.26
1420928_at	*St6gal1*	sialyltransferase 1 (beta-galactoside alpha-2,6-sialyltransferase)	–2.00	–1.69
1415845_at	*Syt4*	synaptotagmin 4	–4.61	–3.07
1450881_s_at	*Tm7sf1*	transmembrane 7 superfamily member 1	–2.83	–2.33
1439255_s_at	*Tm7sf1*	transmembrane 7 superfamily member 1	–2.14	–2.06
1422754_at	*Tmod1*	tropomodulin 1	2.79	26.42
1418935_at	*Trpm1*	transient receptor potential cation channel, subfamily M, member1	–4.26	–4.51
1437531_at	*Trpm1*	transient receptor potential cation channel, subfamily M, member1	–3.01	–3.76
1448361_at	*Ttc3*	tetratricopeptide repeat domain 3	–1.51	–1.75
1448821_at	*Tyr*	tyrosinase	–3.58	–4.39
1456095_at	*Tyr*	tyrosinase	–3.75	–3.17
1417717_a_at	*Tyr*	tyrosinase	–2.95	–3.09
1415862_at	*Tyrp1*	tyrosinase-related protein 1	–3.76	–3.19
1415861_at	*Tyrp1*	tyrosinase-related protein 1	–2.34	–2.56